

1 **Small to large strain mechanical behaviour of an alluvium stabilised with low carbon**  
2 **secondary minerals**

3  
4 P. Sargent\* <sup>1</sup>, M. Rouainia <sup>2</sup> A. Diambra <sup>3</sup>, D. Nash <sup>4</sup> and P. N. Hughes <sup>5</sup>

5  
6 \* Corresponding author

7  
8 1 Stephenson Building, School of Science, Engineering and Design, Stephenson Street, Teesside  
9 University, Middlesbrough, Tees Valley, TS1 3BA, UK.

10 2 Drummond Building, School of Engineering, Newcastle University, Newcastle upon Tyne, Tyne and  
11 Wear, NE1 7RU, UK.

12 3 Queens Building, Department of Civil Engineering, University of Bristol, University Walk, Clifton,  
13 Bristol, BS8 1TR, UK.

14 4 Posthumous. Previous affiliation is Queens Building, Department of Civil Engineering, University of  
15 Bristol, University Walk, Clifton, Bristol, BS8 1TR, UK.

16 5 Christopherson Building, Department of Engineering, Durham University, Lower Mountjoy, South  
17 Road, Durham, DH1 3LE, UK.

18  
19 Paul Sargent MSci MSc PhD CGeol FGS

20 E-mail: p.sargent@tees.ac.uk

21 Tel: +44(0)7815 714237

22  
23 Mohamed Rouainia Dipl. -Ing MSc PhD

24 E-mail: m.rouainia@newcastle.ac.uk

25 Tel: +44(0)191 208 3608

26  
27 Andrea Diambra MEng PhD

28 E-mail: andrea.diambra@bristol.ac.uk

29 Tel: +44(0)117 331 5600

30  
31 David Nash MA MSc DIC PhD MICE CEng

32 E-mail: please forward correspondence to andrea.diambra@bristol.ac.uk

33 Paul N. Hughes BSc MSc PhD

34 E-mail: paul.hughes2@durham.ac.uk

35 Tel: +44(0)191 334 2450

36

## 37 **Abstract**

38 Deep dry soil mixing is a popular ground improvement technique used to strengthen soft compressible soils,  
39 with Portland cement being the most popular binder. However, its continued use is becoming less  
40 sustainable given the high CO<sub>2</sub> emissions associated with its manufacture. Alkali-activated cements are  
41 considered to be viable low carbon alternative binders, which use industrial waste products such as blast  
42 furnace slag. This study focusses on the stabilisation of a potentially liquefiable soft alluvial soil using a  
43 dry granulated binder comprising sodium hydroxide-activated blast furnace slag (GGBS-NaOH). This  
44 binder has previously been demonstrated by the authors to have potential as a replacement for Portland  
45 cement due to its excellent engineering performance, positive contributions towards the circular economy,  
46 reducing energy usage and CO<sub>2</sub> emissions in the construction sector. A detailed comparison in mechanical  
47 behaviour is presented between the soil in its reconstituted, undisturbed and cemented states after 28 days  
48 curing through the use of advanced monotonic triaxial testing techniques, including small strain  
49 measurements. Mechanical behaviour was specifically analysed regarding peak deviatoric strength, pore  
50 pressure response, stress – volumetric dilatancy, shear stiffness degradation over small to large strain  
51 ranges, critical state and failure surfaces. Using 7.5% GGBS-NaOH increased the stiffness and shear  
52 strength of the soil significantly, whereby the shear strains at which initial shear stiffness degrades is three  
53 times higher than the untreated undisturbed soil. As a result, larger amounts of dilation was observed during  
54 shearing of the material and resulted in an upward shift of the soil's original critical state line due to the  
55 creation of an artificially cemented soil matrix through the precipitation of C-(N)-A-S-H gels.

56

## 57 **Keywords**

58 Mechanical behaviour, low carbon, GGBS, alluvium, stiffness degradation, triaxial.

59 **Highlights**

- 60
- Using GGBS in geotechnics contributes towards lowering global CO<sub>2</sub> emissions.
- 61
- GGBS-NaOH stabilisation of a soft soil enhanced strength over various strain levels.
- 62
- Stabilisation successfully delayed the onset of stiffness degradation.
- 63
- The new cemented structure significantly improved the soil frictional behaviour.

64

65 **What is already known in this area?**

66 Extensive research has been undertaken focussing on basic mechanical performance (e.g. UCS) of soils  
67 stabilised with CEM-I binders, which have only been partially replaced by GGBS/PFA.

68

69 **What does this study add to the literature?**

70 Small strain mechanical behaviour of soils stabilised with an alkali-activated GGBS binder, which can  
71 completely replace CEM-I. This has sustainability benefits in terms of lowering CO<sub>2</sub> emissions.

## 72 **1.0 Introduction**

73 Alluvial soils are in great abundance in river flood plains, which are problematic in construction due to  
74 their low bearing capacities and high compressibilities. Deep dry soil mixing (DDSM) has become an  
75 increasingly popular technique for improving such ground conditions. DDSM involves injecting a  
76 cementitious binder into the ground via a rotating auger drill; thereby producing soil-cement columns or  
77 panels. Current trends in the European market also involve using DDSM as an alternative technique for  
78 creating deep pile foundations. DDSM is very versatile in that it may be used to treat a wide variety of soil  
79 types [1], is economical and produces considerably less waste and ground vibration compared with other  
80 ground improvement and piling techniques. Ordinary Portland cement (CEM-I) and lime have been  
81 traditionally used as the cementitious binders in DDSM since this technique was developed in Scandinavia  
82 during the 1960's, due to their favourable strengthening properties.

83 The mechanism through which strength improvements are generally achieved within cement-treated soils  
84 is via an increase in pH conditions and the hydration of calcium silicates / aluminates within the binder to  
85 form cementitious gels, producing a cemented soil matrix. Whilst the majority of strength development  
86 occurs during the first month of curing through hydration, strength continues to increase slowly with time  
87 through pozzolanic reactions if soil  $\text{pH} \geq 10.5$  [2]. To ensure DDSM is effective in enhancing a soil's  
88 engineering performance, it's physico-chemical properties such as particle size distribution, plasticity, pH,  
89 moisture content, cation exchange capacity (CEC), specific surface area, organic and sulphate contents  
90 must be characterised prior to selecting the most appropriate binder. Generally, soils suitable for DDSM  
91 treatment are characterised by low organic contents (<1%), low sulphate contents (<0.3%) and clay contents  
92 of 10–50% [3].

93 The continued use of CEM-I and lime in today's society is becoming less economically and  
94 environmentally sustainable. Cement manufacture is highly energy intensive, requiring 5000MJ per tonne  
95 of CEM-I [4] and contributes up to 7% of the world's CO<sub>2</sub> emissions [5]. To address this issue, efforts have  
96 been made to introduce industrial waste products (IWPs) as partial replacements for CEM-I, including  
97 ground granulated blast-furnace slag (GGBS), pulverised fly ash (PFA), red gypsum (RG) and rice husk  
98 ash (RHA). Alkali-activated cements (AACs) are considered to be popular and viable low carbon and

99 economical alternatives to CEM-I and lime. These materials involve the sole use of pozzolanic aluminosilicate based IWPs in combination with alkalis (e.g. sodium hydroxide, NaOH) for raising soil pH to  
100 promote pozzolanic conditions and activate the hydraulicity of the IWP.  
101

102 There is extensive literature demonstrating that AACs are capable of producing engineering performances  
103 that are either comparable to or exceed those of CEM-I and lime. Cristelo et al. [6] undertook laboratory  
104 and field studies using sodium silicate ( $\text{Na}_2\text{SiO}_3$ )-NaOH activated type F PFA for stabilising a low plasticity  
105 sandy clay. The binder produced higher strengths more rapidly compared with CEM-I stabilised samples.  
106 Sargent et al. [7] assessed the UCS, compressibility, durability and pH performance of NaOH pellet-  
107  $\text{Na}_2\text{SiO}_3$  solution activated GGBS, PFA and RG binders at a dosage of 10% by dry weight to stabilise an  
108 artificial low plasticity alluvial silty sand. Results indicated that alkali-activated GGBS stabilised mixtures  
109 produced the best engineering performances; whereby 28 day UCS of 6MPa was achieved in comparison  
110 to 3MPa achieved by CEM-I stabilised samples. Whilst the activator used promoted pozzolanic conditions,  
111 there are practicality issues associated with using  $\text{Na}_2\text{SiO}_3$  solution in a binder for DDSM. Habert et al. [8]  
112 determined that  $\text{Na}_2\text{SiO}_3$  production is also more expensive and has a higher environmental impact than  
113 NaOH. Bernal [9] determined that  $\text{Na}_2\text{SiO}_3$  has a higher accelerated carbonation depth over NaOH. These  
114 findings informed Sargent et al.'s [10] study for treating a soft alluvium from Northumberland (UK),  
115 whereby the binder used was GGBS-NaOH, with a GGBS-NaOH ratio of 2:1 at dosages of 0 – 10% by dry  
116 weight. Whilst a 10% dosage produced the best engineering performances, using a 7.5% dosage was  
117 sufficient for achieving EuroSoilStab (2002) [12] 28 day undrained shear strength requirement of 150kPa.  
118 The 7.5% dosage also produced strengths that were superior than using 10% CEM-I and was deemed more  
119 economically and environmentally sustainable.

120 With the progressive closure of coal fired power stations and extensive use of PFA in concretes and grouts  
121 over the past few decades as a partial replacement for CEM-I, PFA supplies are rapidly disappearing –  
122 especially in the UK. Hence, the future development of AACs needs to utilise IWP waste streams which  
123 have longevity in supply. Whilst the UK steel manufacturing industry is declining, other global economies  
124 (e.g. China, USA) continue to grow – particularly in the construction sector. Hence, the demand for steel  
125 continues to rise meaning that slag waste will continue to be produced worldwide for the foreseeable future.  
126 Slags produced from steel manufacture represent approximately 15% by mass of the steel produced [12].

127 This highlights the continued need to recycle slag to make positive contributions towards the circular  
128 economy and reducing global CO<sub>2</sub> emissions.

129 Other recent studies that have investigated alternative waste streams for developing AACs in soil  
130 stabilisation include NaOH-activated volcanic ash (VA) to stabilise a low plasticity clay [4]. Whilst VA is  
131 naturally pozzolanic, represents a vast worldwide resource and when NaOH-activated produces strengths  
132 200% higher than CEM-I stabilised samples [4], there are potential environmental implications. These  
133 include the need to quarry out ash deposits and that VA can contain elevated concentrations of Cl, S and F  
134 [14], all of which are water-soluble. Depending on the geological setting in which VA is produced, it may  
135 be highly acidic or alkaline and have knock-on effects on the pH of surface waters. Collectively, these could  
136 have negative impacts on soil fertility, groundwater resources and associated ecosystems if VA cements  
137 are used in DDSM.

138 Whilst there is extensive literature covering laboratory investigations into the performance of IWP, CEM-  
139 I and AAC concretes that focus on unconfined compressive strength, there is relatively little material which  
140 investigates their mechanical behaviour in the context of geotechnical materials over small to large strain  
141 ranges using triaxial equipment. Ahnberg [15] undertook triaxial tests on two Swedish clays stabilised with  
142 lime, CEM-I and GGBS at a dosage of 100kg/m<sup>3</sup>. Whilst Ahnberg observed variations in shear strengths  
143 due to the soil type, binder design and curing period, stress-strain behaviour was noted to be similar due to  
144 the degree of overconsolidation. Rios et al. [16] investigated the shearing behaviour of a CEM-I stabilised  
145 silty sand, derived from weathered Porto granite. Triaxial testing was undertaken over a range of confining  
146 pressures (30 – 20,000kPa), whereby samples were prepared with controlled binder dosages of 2 – 7%. In  
147 both effective deviatoric and volumetric stress spaces, Rios et al. [16] identified a possible critical state line  
148 (CSL) for the cemented soil at large strains – independent of the binder dosage or porosity/cement index.  
149 Additionally, Rios et al. [16] concluded that normal compression lines (NCL), CSL and state boundary  
150 surface for the cemented soil may be independent of binder dosage but may depend only on binder dosage  
151 in terms of porosity/cement ratio.

152 Knowledge of how soft soils and cement stabilised soils behave at small strain levels is of key interest in  
153 geotechnical design when considering soil–structure interactions for foundations and retaining walls.  
154 Presented in this paper are results from a suite of drained and undrained isotropically consolidated triaxial



155 compression tests undertaken on an alluvium in its natural undisturbed state, reconstituted state and when  
 156 treated with a GGBS-NaOH binder after 28 days curing. Tests were undertaken over a range of effective  
 157 stress conditions to understand the improvement in mechanical behaviour achieved when using an optimum  
 158 binder dosage. Testing data is presented in terms of small strain shear stiffness degradation, critical state  
 159 and stress dilatancy.

160

161 **2.0 Materials and Testing Methodologies**

162 2.1 Soil and Binder Materials

163 2.1.1 Lanton Alluvium

164 The alluvial soil considered in this study was sourced from the River Glen flood plain in Lanton,  
 165 approximately 4km North West of Wooler in Northumberland, UK. Disturbed and undisturbed thin-walled  
 166 U100 samples were taken from the depth range of 1.5–2.4m. The local superficial geology is characterised  
 167 by Holocene alluvium deposits along the course of the River Glen, bounded by river terrace sand and gravel  
 168 deposits, Devensian glacial till and fluvioglacial deposits. The index properties of the soil were determined  
 169 by Sargent et al. [10], which are summarised in Table 1. A soil grading curve and compaction curves for  
 170 the Lanton alluvium soil are provided in Figures 1 and 2 respectively. The particle size distribution and  
 171 compaction curves for the soil were obtained using methods in accordance with BS1377 [11].

172

173 Table 1: Summary of the Lanton alluvium’s index properties. Sourced from Sargent et al. (2016).

Property	Unit	Value
In-situ moisture content	%	25
Plasticity Index	%	14.95
Liquid Limit	%	35.66
Saturated unit weight	kN/m <sup>3</sup>	18.44
Bulk Density	Mg/m <sup>3</sup>	2.0
Dry density	Mg/m <sup>3</sup>	1.74
Cation exchange capacity	cmol/kg	11.45
Specific surface area	m <sup>2</sup> /g	6.45
Total organic content	%	0.76
Sulphate content	mg/kg soil	49
BS 5930 (BSI, 1990) classification	-	Silty SAND

174

175

176

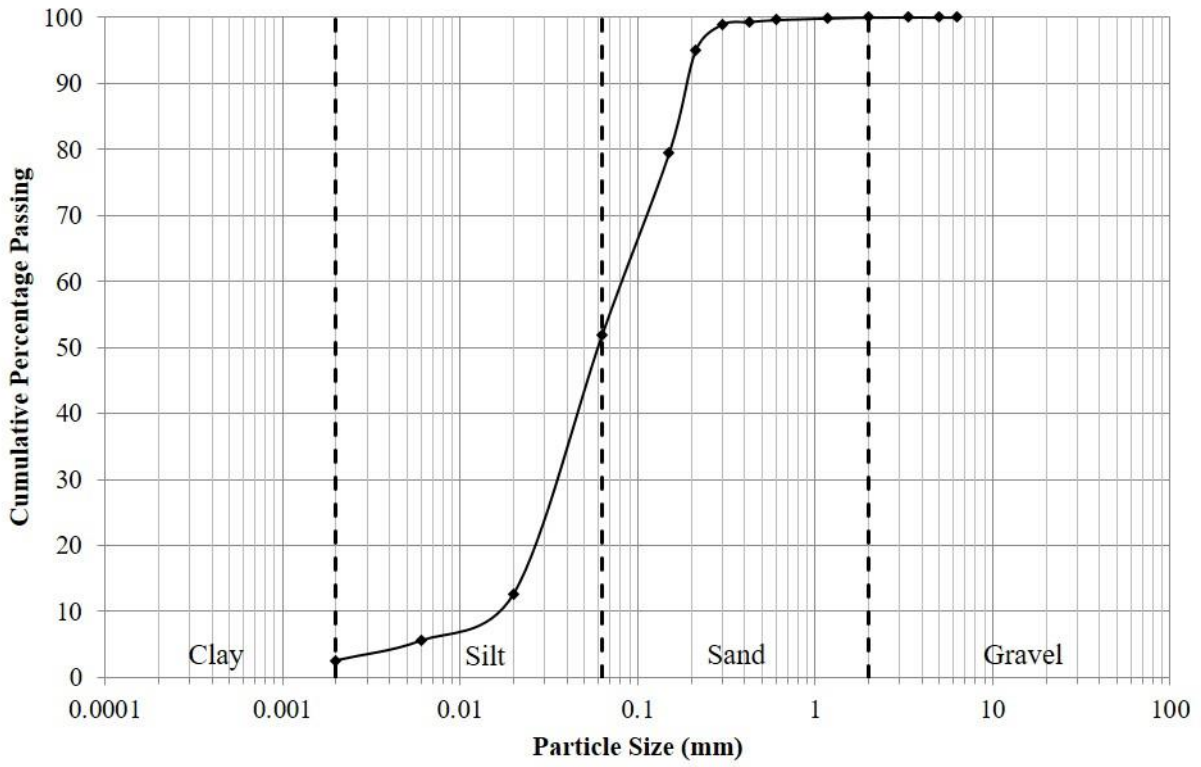


Figure 1: Soil grading curve for Lanton alluvium.

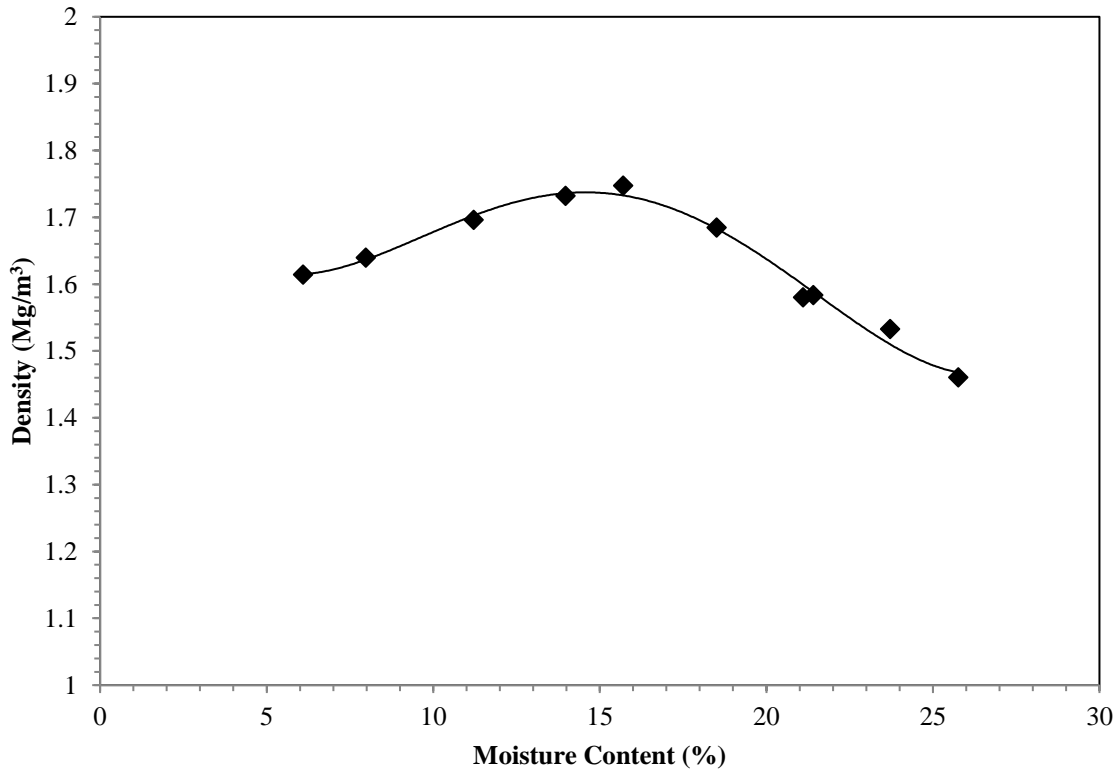


Figure 2: Dry density compaction curve for Lanton alluvium.

### 2.1.2 Cementitious Binder

The dry binder and dosage used was based on the results from Sargent et al. [10]. The IWP used was GGBS as supplied by Hanson Cements Ltd., which was mixed with NaOH in dry pellet form (supplied by Fisher

186 Scientific UK Ltd) as an alkali activator. The molarity of the NaOH was 39.997g/mol. Sargent et al. [10]  
187 revealed that an optimum dosage of 7.5% by dry weight is appropriate for stabilising Lanton alluvium, with  
188 a view to achieving engineering performances which are comparable or exceed those of Lanton alluvium  
189 stabilised with lime or CEM-I. Additionally, the 7.5% dosage of GGBS-NaOH ensured that the stabilised  
190 alluvium met the minimum 28 day undrained shear strength requirement of 150kPa defined by  
191 EuroSoilStab [12]. Hence, this is the binder design selected for this study.

192

## 193 2.2 Testing Methodologies

194 To gain a comprehensive understanding of the short and long term mechanical behaviour of reconstituted,  
195 undisturbed and GGBS-NaOH treated Lanton alluvium, particularly in defining their respective critical  
196 state lines, yield surfaces and effective shear strength properties; monotonic consolidated drained and  
197 undrained triaxial tests were undertaken under a minimum of four effective confining stress conditions.  
198 Bender elements and local instrumentation were employed to characterise the initial shear stiffness of the  
199 material over a range of stress level and its degradation during shearing.

200

### 201 2.2.1 Sample Preparation

#### 202 2.2.1.1 Reconstituted samples

203 Cylindrical samples 100mm in diameter and 200mm long were prepared by initially drying the disturbed  
204 soil in an oven at 110°C for 24 hours. Once dry, the soil was milled into a fine powder (particle size  $\leq 1\text{mm}$ )  
205 for ease of sample mixing and then mixed with water in a Hobart rotary mixer for 10 minutes to achieve a  
206 gravitational moisture content of 25% (per the soil's in-situ moisture content) and homogeneity. Once  
207 mixed, the soil was compacted into three layers within a standard 100mm diameter compaction mould in  
208 accordance with BS 1377 [11]. All samples were prepared with a bulk density of  $1.75\text{Mg/m}^3$ , based on  
209 optimum compaction criteria. Once compacted, the sample was extruded and trimmed in preparation for  
210 triaxial testing according to BS1377 [11]. Prior to placing on the triaxial base pedestal and encapsulation  
211 within a latex membrane, sample masses and dimensions were measured. Due to the soil's high silt content,

212 low cohesion, relatively high moisture content and absence of natural internal structure, reconstituted  
213 samples displayed some slumping upon extrusion.

214

#### 215 2.2.1.2 Undisturbed Thin-walled (UT) samples

216 100mm diameter UT100 sized samples were obtained from the field, wax sealed and wrapped in bubble  
217 wrap to prevent loss of moisture and minimise sample disturbance during transport to the laboratory. Prior  
218 to mounting on the triaxial base pedestal for testing, samples were extruded and trimmed to the appropriate  
219 dimensions, weighed on a mass balance and dimensions measured. Undisturbed samples exhibited little  
220 slumping upon extrusion compared with reconstituted samples, thereby providing an indication of the soil's  
221 initial sedimentation structure.

222

#### 223 2.2.1.3 Alkali activated cemented samples

224 For practicality purposes in the laboratory, maximising sample homogeneity and the number of reactive  
225 sites for cementitious bond formation, samples were prepared in accordance with the methodology adopted  
226 by Sargent et al. [10] by first mixing the oven dried soil powder with the GGBS-NaOH binder at a dosage  
227 of 7.5% by dry weight in a rotary mixer for 10 minutes. The GGBS – NaOH ratio used was one part NaOH  
228 to two parts GGBS [10]. Once the required quantities of soil and binder had been mixed, water was  
229 incrementally added to the mixture to achieve the pre-treatment (in-situ) soil optimum moisture content of  
230 25%. Samples were tamped and compressed into a split sample mould, inserted into a hydraulic press to  
231 form samples of various sizes (200mm long – 100mm diameter; 100mm long – 50mm diameter; 76mm  
232 long – 38mm diameter) and achieve a target density of  $1.9\text{Mg/m}^3$  based on optimum compaction criterion.  
233 Samples were then cured within wax-sealed PVC tubes for 28 days [17] and stored within a temperature-  
234 controlled room with a relative humidity of 55% and ambient air temperature of  $20^\circ\text{C}$  [7] [10]. Once cured  
235 and extruded, sample ends were carefully trimmed using a surface grinder within a tolerance of  $25\mu\text{m}$   
236 according to ASTM D4543-08 [18]. This ensured sample ends were smooth, parallel with each other and  
237 reduced bedding errors during testing.

238

## 239 2.2.2 Apparatus and Testing procedures

240 Triplicate samples of each material were tested for each effective confining stress to remove bias, identify  
241 anomalies and maximise data reliability. Table 2 summarises the triaxial testing programme undertaken. A  
242 total number of 53 triaxial tests were performed.

243

244 Table 2: Experimental programme for triaxial testing

Sample ID Convention	Sample type	Drainage condition	GGBS-NaOH content (%)	Effective mean confining stress, $p'_0$ (kPa)
ReconCU X <sup>[1]</sup> _Y <sup>[2]</sup>	Reconstituted	Undrained	0	50, 100, 150, 250
ReconCD X_Y	Reconstituted	Drained	0	50, 150, 200
UndisCU X_Y	Undisturbed	Undrained	0	50, 150, 250
UndisCD X_Y	Undisturbed	Drained	0	50, 150, 200
CemCU X_Y	28 day Cemented	Undrained	7.5	50, 100, 200, 300, 400, 600
CemCD X_Y	28 day Cemented	Drained	7.5	50, 100, 200, 400, 600

245 Notes: [1] – Value for ‘X’ denotes the  $p'_0$  value used for the test. [2] – Value for ‘Y’ denotes the test sample number.

246

### 247 2.2.2.1 Apparatus

248 The equipment used comprised a 2MPa capacity perspex cell mounted on an electro-mechanical advanced  
249 digital triaxial system. A 64kN capacity submersible load cell was mounted on the end of the loading ram  
250 within the triaxial cell. Cell pressures were controlled and regulated via a 3MPa digital pressure controller,  
251 whereas a 1MPa digital pressure controller was used to supply and control back pressures and monitoring  
252 sample volume changes. To accurately measure the cell pressure, back pressure and pore pressures at the  
253 top and base of samples during tests, calibrated 15 bar capacity pressure transducers were fitted to the base  
254 of the triaxial cell. An external LVDT was mounted on the exterior of the triaxial cell to measure external  
255 ram displacements. For measuring local axial strains ( $\epsilon_a$ ) on samples, two LVDT local strain gauges were  
256 mounted diametrically opposite each other to the middle third section of samples which is considerably less  
257 restrained compared with the sample ends. A further LVDT local strain gauge was used to measure radial  
258 strains at mid-sample height, which was mounted via a radial caliper. To accurately measure changing shear  
259 stiffnesses during shearing over the small to large strain range, bender elements were installed within the  
260 sample top cap and triaxial frame base pedestal.

## 262 2.2.2.2 Triaxial Testing Procedures

263 When mounting untreated soil samples within the triaxial cell for testing, bender elements installed within  
264 the top cap and base pedestal protruded by 10mm, which ensured they were of sufficient length to penetrate  
265 through the porous discs and then pressed by hand into the sample ends by 3–5 mm – ensuring a good  
266 contact. However, for cemented samples the bender elements could not simply be pushed in by hand.  
267 Instead, 5mm deep slots were formed in the sample ends by using a Stanley knife. To ensure good coupling  
268 between the cemented samples and the bender elements, any gaps between the slot walls and the bender  
269 elements were infilled by using a filler made from the Lanton alluvium – GGBS-NaOH mixture. The top  
270 cap was then directly connected to the submersible load cell to reduce bedding errors. After filling the  
271 triaxial cell with de-aired water, samples were saturated in general accordance with BS1377 [11]. Cell and  
272 pore pressures were incrementally increased by 50-100kPa per day until a minimum back/pore pressure of  
273 350kPa was achieved to ensure dissolution of air bubbles within the back pressure system. An effective  
274 confining stress of 5-10kPa was maintained throughout saturation. Samples were considered saturated once  
275 a minimum Skempton's B value of 0.95 was recorded. Following saturation, samples were isotropically  
276 consolidated until the required effective confining stress ( $p'_0$ ) had been reached and the volume change  
277 stabilised. The  $p'_0$  conditions used for tests are summarised in Table 2. Throughout saturation and  
278 consolidation stages, the submersible load cell maintained a constant deviatoric stress ( $q$ ) on the sample of  
279 0kPa to reduce bedding errors and enabled the constant measurement of changing sample height throughout  
280 tests. After consolidation, samples were compressed at constant  $\epsilon_a$  rates of 0.01mm/minute and  
281 0.05mm/minute for undrained and drained tests respectively, based on BS1377 [11] calculations. The  
282 failure criteria selected for this work were peak effective stress ratio and ultimate state (i.e. reaching  $\epsilon_a$  of  
283 15%) to capture the residual (i.e. critical state) mechanical behaviour of samples.

284 At the end of saturation, consolidation and during compression stages of each test, bender element  
285 measurements were taken to determine degradations in sample shear stiffnesses. An S-wave was  
286 transmitted from the bender element housed within the sample top cap, through samples and received by  
287 the bender element within the base pedestal. A minimum of three wavelengths were required to pass through

288 samples during bender element tests. The frequency used for the source bender element's signal bursts was  
289 based on prior knowledge of the stiffness of the Lanton alluvium in its untreated and cemented states, in  
290 addition to a sensitivity analysis whereby frequency was varied between 1 and 50kHz to identify which  
291 frequency produced the highest quality S-wave signal. It was determined that S-wave signals produced for  
292 bender element measurements using lower frequencies were characterised by higher degrees of noise, due  
293 to the influence of the near field effect [19]. The optimum frequency for bender element measurements  
294 taken for all sample types was found to be 20kHz. The time domain method for determining S-wave arrival  
295 times from bender element tests was adopted, which assumes no reflected/refracted waves are detected.  
296 The arrival of the received signal tends to be characterised by an initial downward deflection relative to the  
297 travel time (x) axis, which arises from the "near field effect". This effect is caused by wave front spreading  
298 and coupling between waves that are characterised by similar particle motions but propagating at different  
299 velocities [19] [20]. The GDS BEAT tool was predominantly used as a convenient method for analysing  
300 the bender element data sets, by using the time and frequency domain techniques. Based on the experience  
301 of the authors in the use and interpretation of bender elements, the first bump maximum was considered  
302 the most suitable point on the received signal as the first S-wave arrival. Figures 3 and 4 show the  
303 experimental apparatus used for taking bender element measurements and some representative S-wave  
304 signals observed for the untreated and GGBS-NaOH treated Lanton alluvium, respectively.

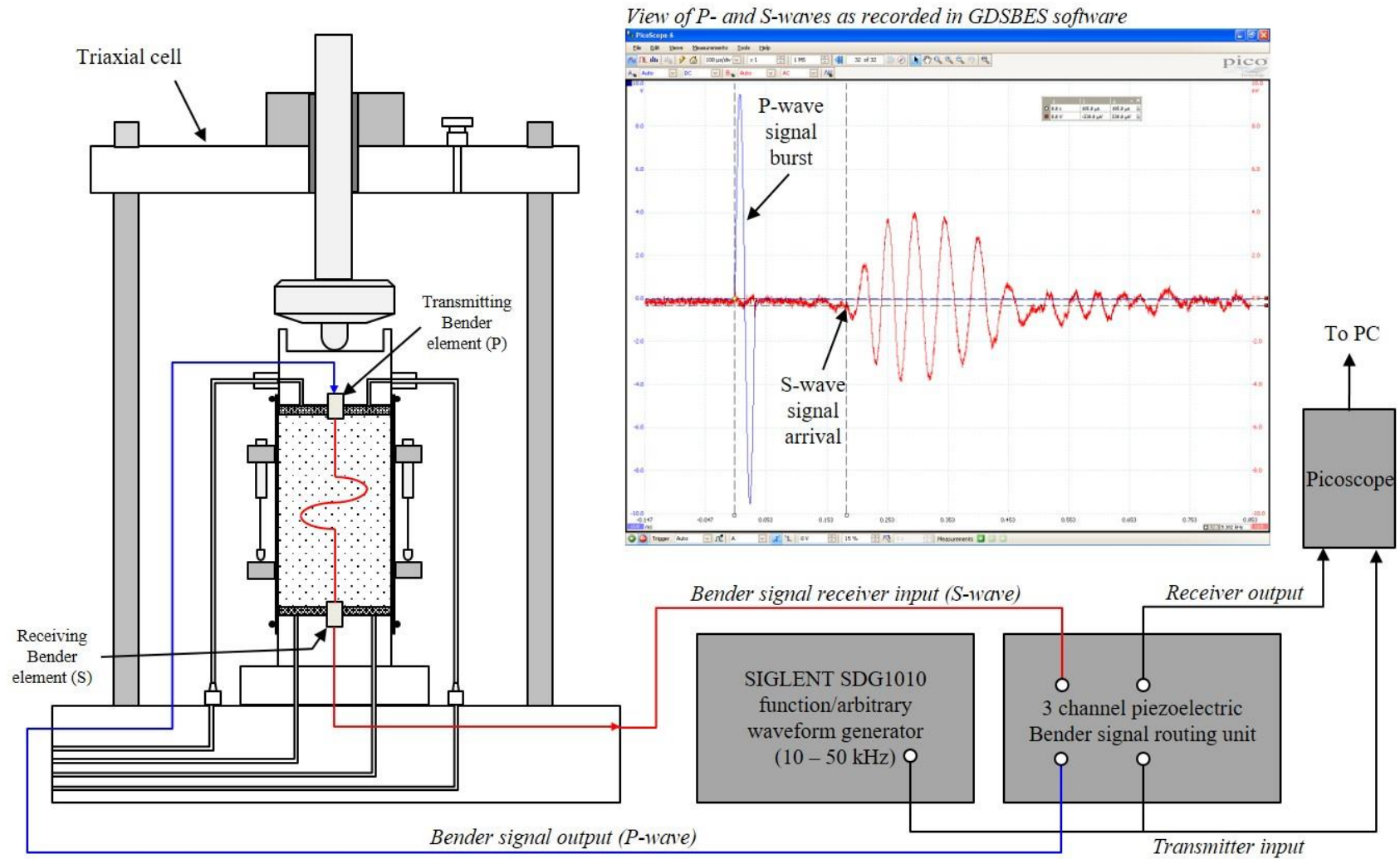
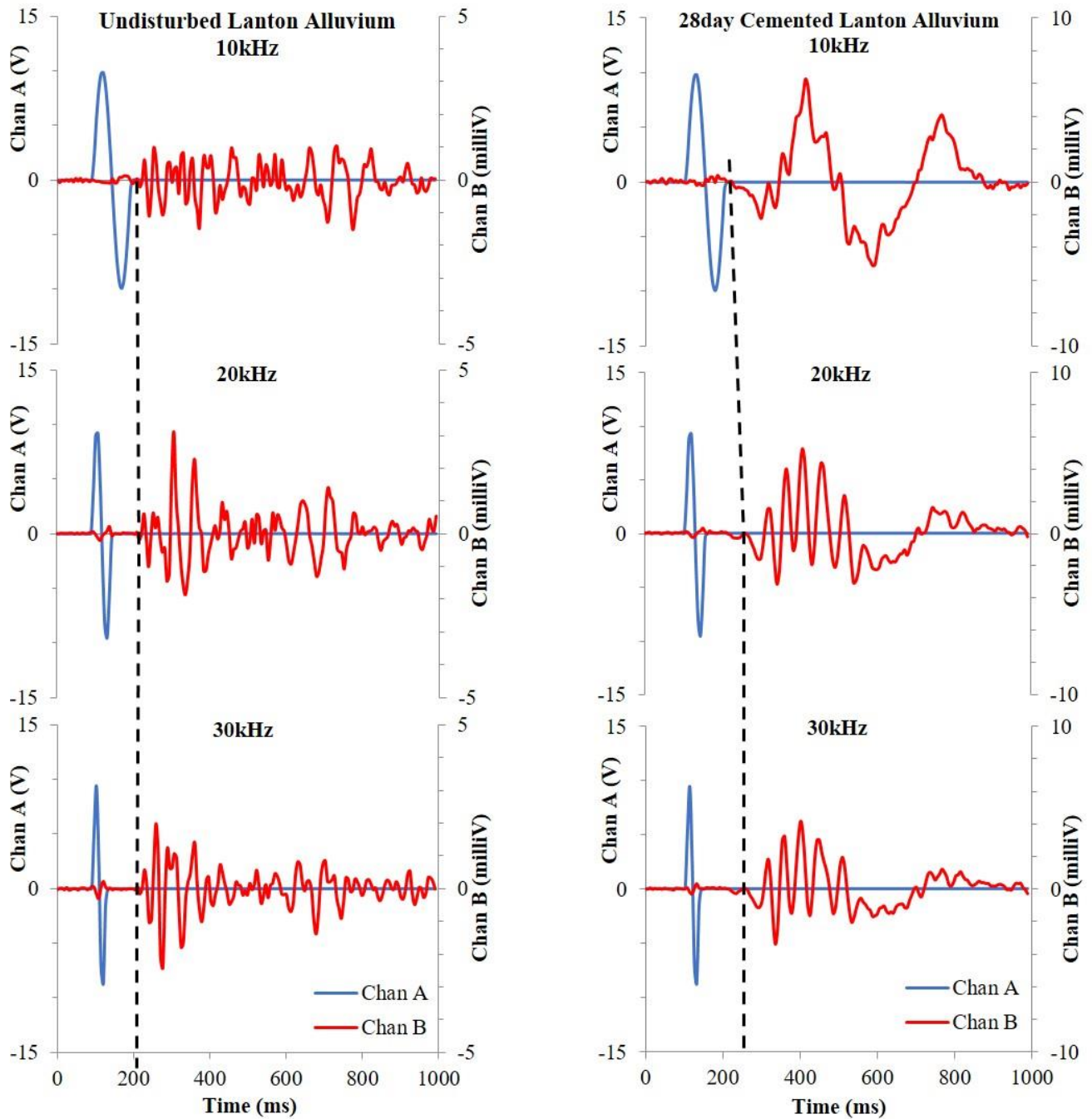


Figure 3: Bender element apparatus used within triaxial apparatus.





309

310 Figure 4: Source and received signals recorded for bender element measurements taken at frequencies of 10-30kHz during  
 311 triaxial tests on samples of undisturbed Lanton alluvium (left) and 28 day GGBS-NaOH stabilised Lanton alluvium (right).

312

### 313 3.0 Results

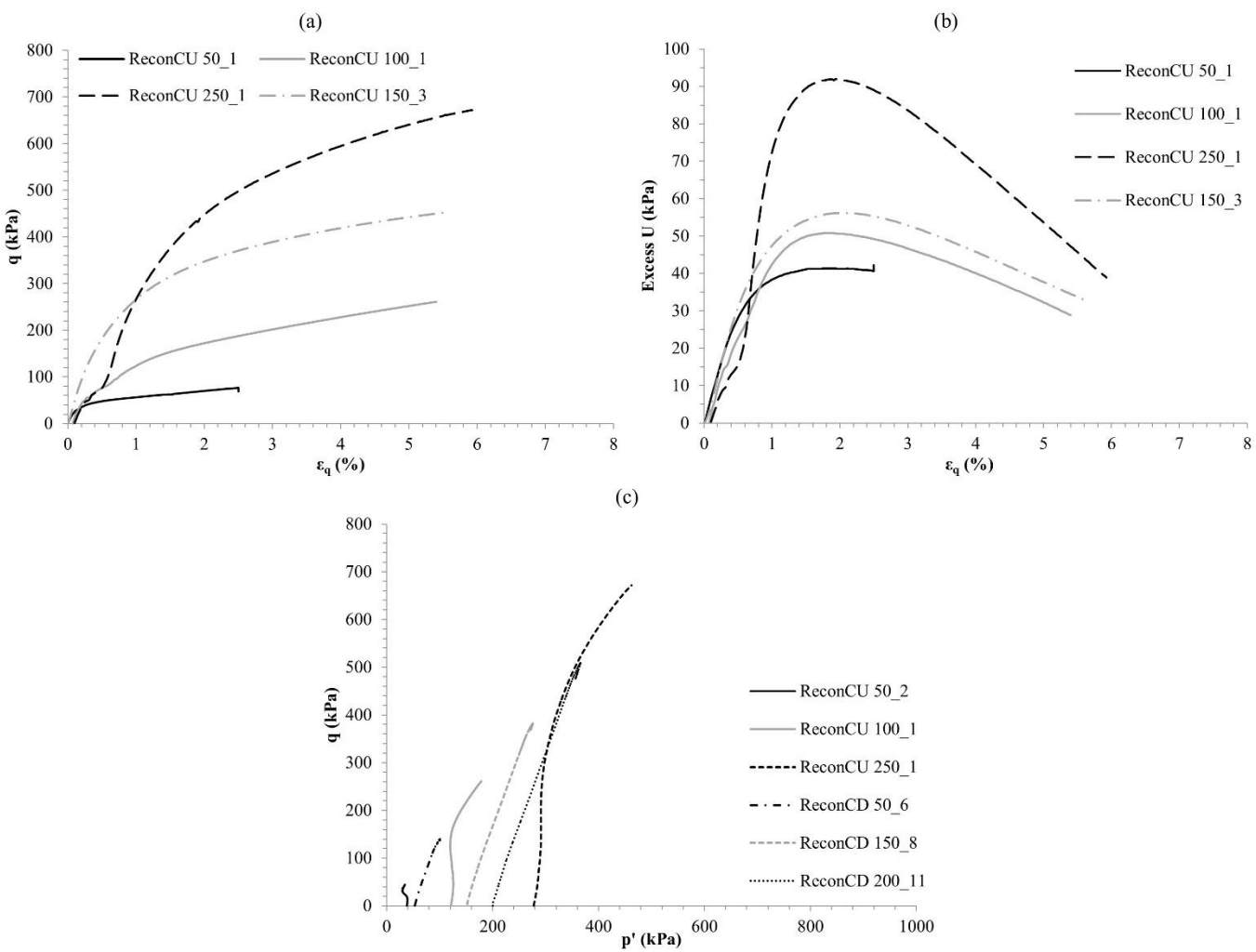
#### 314 3.1 General stress-strain behaviour

##### 315 3.1.1 Reconstituted Lanton alluvium

316 The mechanical response under consolidated undrained triaxial shearing of the reconstituted samples are

317 displayed in Figure 5 in terms of  $q$ - $\epsilon_a$  response (Figure 5a), excess pore pressure ( $U$ ) - deviatoric strain ( $\epsilon_q$ )

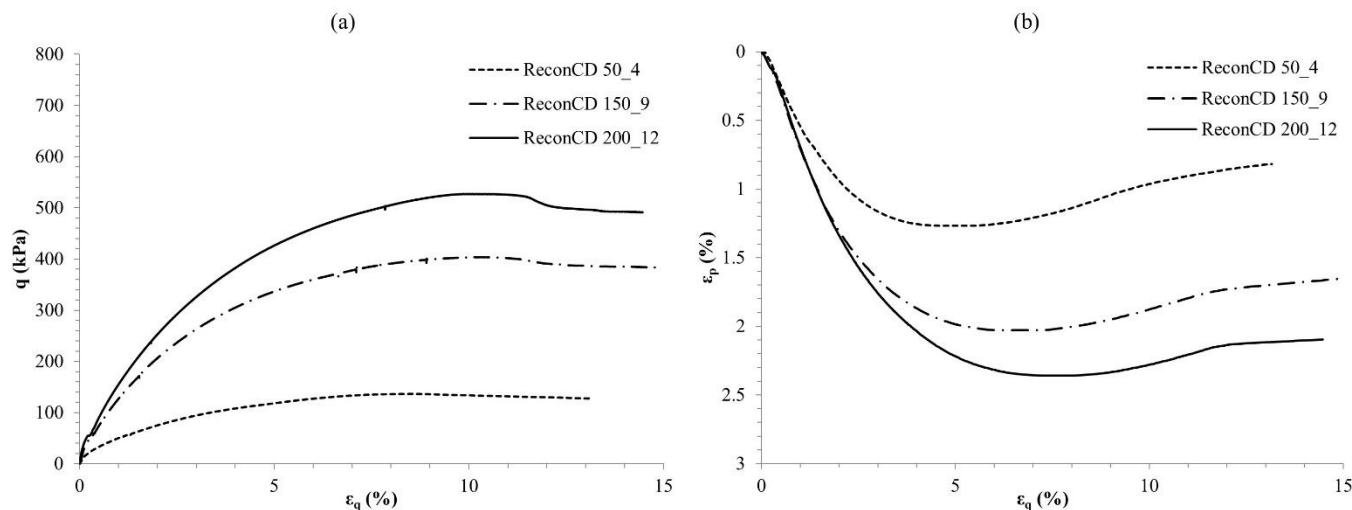
318 response (Figure 5b) and  $q$  versus mean isotropic stress (Figure 5c). The undrained  $q$ - $\epsilon_a$  behaviour of the  
 319 reconstituted alluvium all exhibited work hardening up to peak strength at deviatoric strains of 5–6%.  
 320 Irrespective of the confining stress level, ranging from 50–250kPa,  $U$  shows a pronounced tendency to  
 321 contraction with increases in the applied confining stress. For  $p'_0=50$ kPa, pressures increased up to 20–40  
 322 kPa at  $\epsilon_q$  of 1%; where pressures equalised with further straining until failure. In contrast,  $U$  values within  
 323 undrained samples tested at  $p'_0=100$ –250kPa reached peak values of 50–90kPa at 2%  $\epsilon_q$ . With increasing  
 324  $\epsilon_a$ , a gradual reduction in  $U$  of 30–50kPa was then observed until failure.



325  
 326 Figure 5: (a) Undrained deviatoric stress – strain response; (b) excess pore pressure – deviatoric strain response and (c) drained  
 327 and undrained effective stress paths in the deviatoric stress – mean isotropic stress plane for reconstituted Lanton alluvium  
 328 during shear tests.

329  
 330 The  $q$  and volumetric response of reconstituted samples under drained conditions with increasing  $\epsilon_q$  is  
 331 presented in Figure 6. Most samples sheared under initial effective stresses of 50 and 150kPa displayed  
 332 work hardening between small and large strains up to failure. However, at  $p'_0$  values of 200–250kPa

333 samples exhibited some limited evidence of strain softening at larger strains (>10% for drained tests). Along  
 334 with the contractive behaviour typical of normally consolidated samples, the volumetric response shows  
 335 an overall compressive behaviour as observed in Figure 6b. Compressive behaviour increased with  
 336 confining cell pressure and very limited dilation of 0.2% at large strains only.



337

338 Figure 6: (a) Drained deviatoric stress – shear strain and (b) dilational behaviour of reconstituted Lanton alluvium during shear  
 339 tests.

340

341 For drained tests undertaken at  $p'_0 = 50, 150$  and  $200$  kPa, peak dilation occurred at  $\epsilon_q$  values corresponding  
 342 to peak strength. Upon reaching  $\epsilon_q$  of 12–15% where most samples reached their final  $q$  value, dilation  
 343 became suppressed, suggesting that most samples had reached their critical state. Volumetric trends for the  
 344 samples tested are seen tending towards zero volumetric strain ( $\epsilon_p$ ). Strain localisation or shear plane  
 345 development were generally not observed for reconstituted samples.

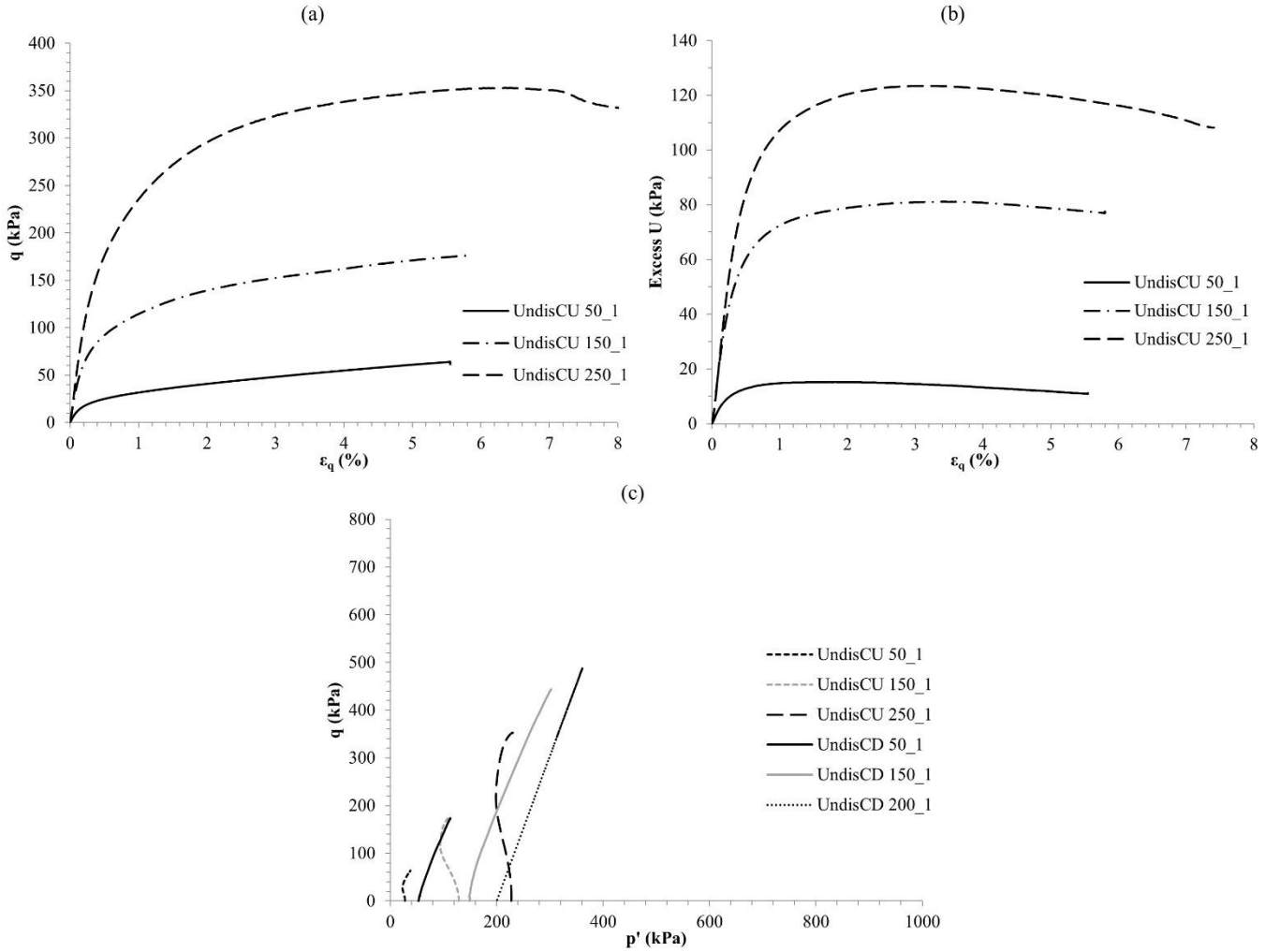
346 Using the slope ( $M^*$ ) from the dilation segments of the  $\epsilon_p$ – $\epsilon_q$  curves in Figure 6b, dilation angles ( $\psi$ ) values  
 347 for the reconstituted material generally ranged between  $1.37$ – $1.81^\circ$ . Higher  $\psi$  values of up to  $2.3^\circ$  were  
 348 recorded in some samples, which may be attributable to slight density variations between samples.

349

### 350 3.1.2 Undisturbed Lanton alluvium

351 The typical mechanical responses for undisturbed Lanton alluvium samples are reported in Figure 7 in  
 352 terms of undrained  $q$  versus  $\epsilon_q$  (Figure 7a),  $U$  versus  $\epsilon_q$  (Figure 7b) and  $q$  versus mean isotropic stress ( $p'$ )  
 353 (Figure 7c). The undrained  $q$ – $\epsilon_q$  behaviour of undisturbed samples consolidated to  $p'_0=50$  and  $150$  kPa

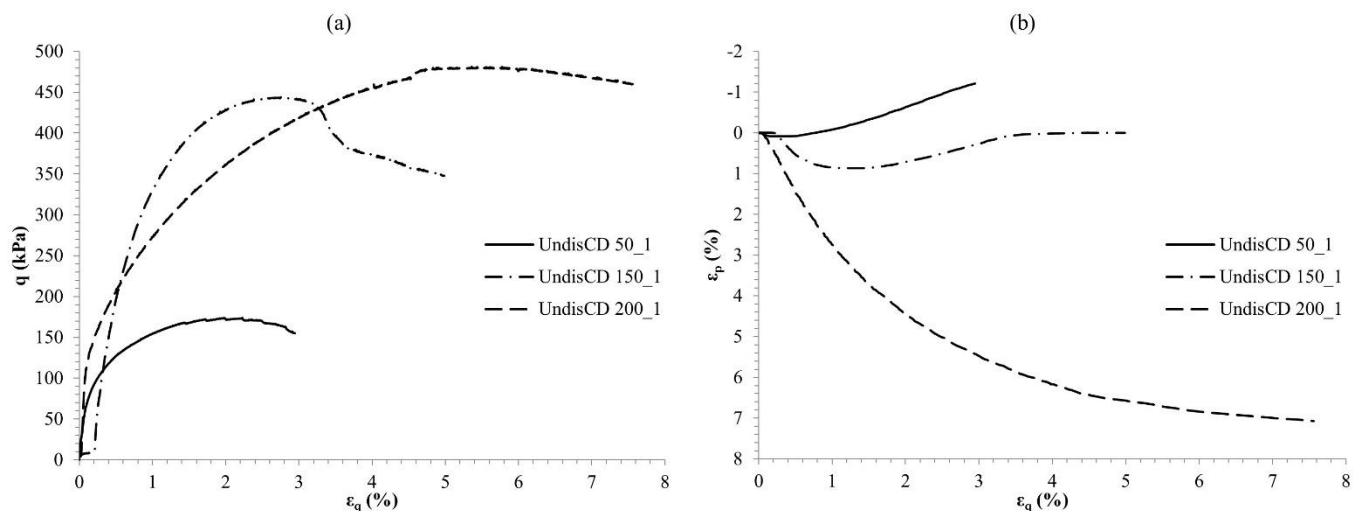
354 displayed work hardening up to failure. Whereas samples consolidated to  $p'_0=250\text{kPa}$  experienced strain  
 355 softening at strains  $>7\%$ . In general, it can be seen from Figures 5a and 7a that the peak  $q$  achieved for  
 356 reconstituted samples were markedly higher than those for undisturbed samples. This apparent higher  
 357 strength is likely due to a degree of over-compaction during preparation of reconstituted samples.



358  
 359 Figure 7: (a) Undrained deviatoric stress – strain response; (b) excess pore pressure – deviatoric strain response and (c) drained  
 360 and undrained effective stress paths in the deviatoric stress – mean isotropic stress plane for undisturbed Lanton alluvium  
 361 during shear tests.  
 362

363 The  $U$  trends show a general increase with strain, with a peak reached between 1.5 and 3%  $\epsilon_q$ , followed by  
 364 a slow reduction under further straining. However, with continued shearing post-peak,  $U$  slightly increased  
 365 before equalising. This behaviour coincides with the onset of strain localisation and softening. Compared  
 366 with reconstituted samples, it appears that slightly larger build ups were observed for undisturbed samples.  
 367 During the consolidated drained triaxial tests, as reported in Figure 8, work hardening is observed up to  
 368 approximately 2–2.5%  $\epsilon_q$  for samples consolidated and tested at  $p'_0$  of 50–150kPa. This was followed by a

369 pronounced period of strain softening, most likely resulting from the damage of the natural soil structure  
 370 during shearing. The sample UndisCD 200\_1 tested at a higher confining stress exhibited a much more  
 371 limited softening response, showing work hardening behaviour up to approximately 5%  $\epsilon_q$ .



372

373 Figure 8: (a) Drained deviatoric stress – shear strain and (b) dilational behaviour of reconstituted Lanton alluvium during shear  
 374 tests.

375

376 Strain localisation and shear plane development were observed within all undisturbed samples. Based on  
 377 the soil's OCR of 1 obtained from oedometer testing [21], Lanton alluvium is considered normally  
 378 consolidated.  $p'_{0}$  normalised undrained elastic stiffness ( $E_{u,p'0}$ ) and drained elastic stiffness ( $E'_{p'0}$ ) for the  
 379 undisturbed soil were recorded as  $E_{u,p'0} = 63\text{--}139\text{MPa}$  and  $E'_{p'0} = 166\text{--}600\text{MPa}$ . The undrained stiffnesses  
 380 were lower and drained stiffnesses were higher compared with those recorded for the reconstituted soil;  
 381 namely  $E_{u,p'0} = 223\text{--}297\text{MPa}$  and  $E'_{p'0} = 150\text{--}215\text{MPa}$ . The slightly higher stiffness values recorded for the  
 382 undrained reconstituted samples are likely to be attributed to considered to a degree of over-compaction  
 383 during sample preparation. From these figures, it is clear that  $p'_{0}$  conditions used during testing influences  
 384 the elastic moduli. Furthermore, considering the higher yield stresses of undisturbed samples over  
 385 reconstituted samples, the post-yield softening behaviour can be attributed to the degradation of the bonding  
 386 based sedimentation structure within the soil. During drained tests, higher peak  $q$  values were noted  
 387 compared with reconstituted samples due to their internal structure which would have caused dilation. Once  
 388 the peak  $q$  had been reached, softening was observed.

389 The radial stiffness of some undisturbed samples as measured from local strain gauges appeared higher  
390 than their axial stiffness, which in turn produced a Poisson's ratio ( $\nu$ ) of approximately 0.33. Such a value  
391 is typical for a soft silty alluvial soil, whereby Bowles [22] stated that  $\nu$  values of 0.3–0.35 may typically  
392 be expected. This observation may indicate a degree of stiffness anisotropy within the soil. Further testing  
393 with horizontally mounted bender elements at the centre of samples would be required to investigate this  
394 postulate.

395 As for reconstituted samples, higher degrees of dilation were observed within samples which had been  
396 consolidated to lower  $p'_0$  values. Figure 6b shows that for tests conducted at  $p'_0=50$  and 150kPa, dilation  
397 initiated at much smaller shear strains of 0.3 and 1.2% respectively, compared with reconstituted samples.  
398 At these strain levels, samples were generally within 1%  $\epsilon_q$  of reaching their yielding points, indicating that  
399 samples stress paths were close to the CSL. The sample tested at  $p'_0=50$ kPa reached maximum effective  
400 stress ratio and therefore failure at  $\epsilon_q = 3\%$ .

401 The contraction experienced by sample UndisCD 200\_1 became negligible with further straining at  $\epsilon_q >6\%$ .  
402 The dilation coupled with loss of structure may explain the observed post-yielding softening behaviour for  
403 samples UndisCD 50\_1 and UndisCD 150\_1 [23].

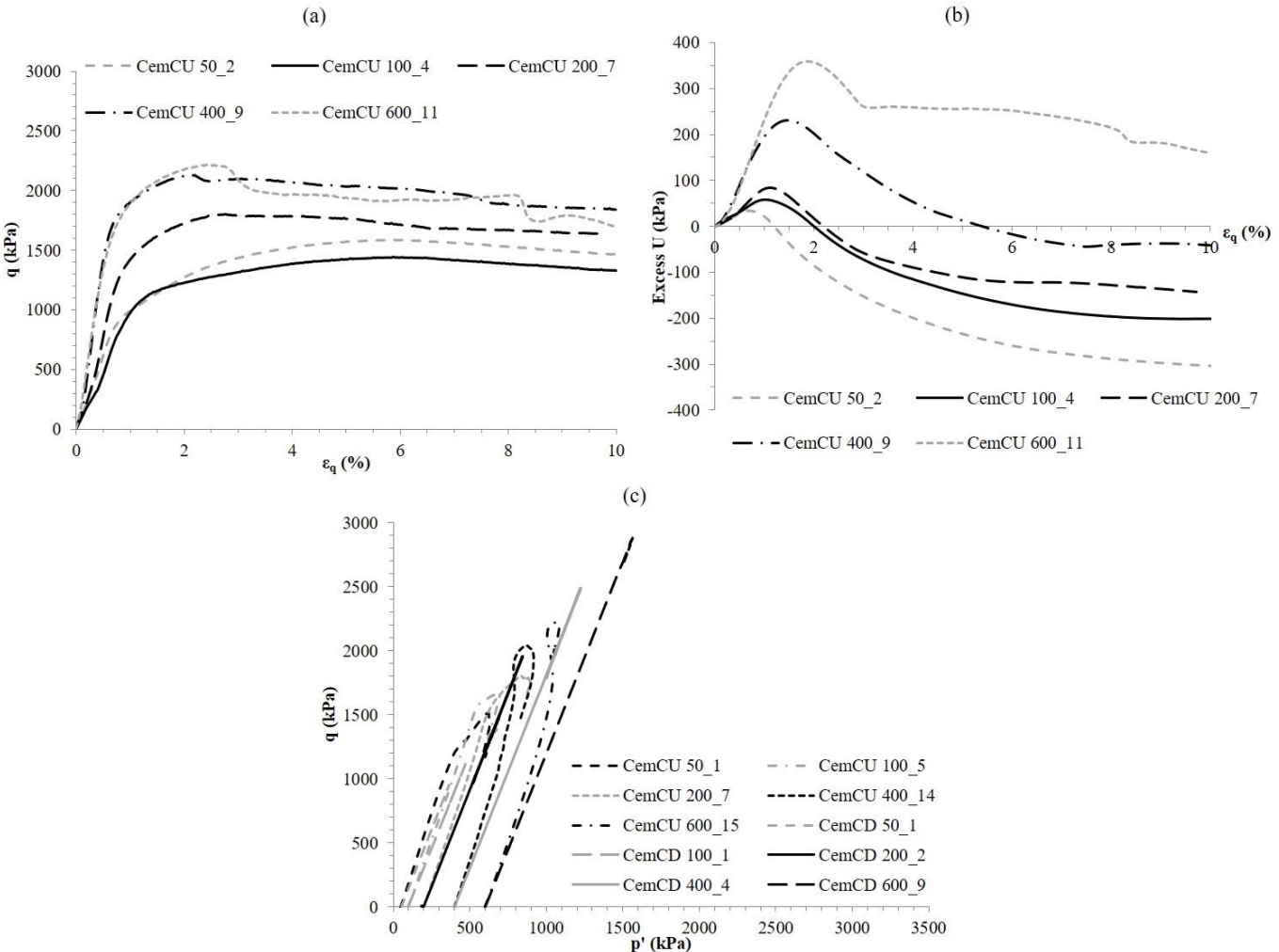
404  $\Psi$  values were calculated to range between  $4.2\text{--}13.6^\circ$ , whereby such variation confirms that higher  $p'_0$   
405 values inhibit soil particle rearrangement. Based on the typical friction angle value of  $33^\circ$  for loose silty  
406 sand as given by Carter and Bentley [24] and the formula of  $\psi = \phi - 30$ , the  $\psi$  values measured for Lanton  
407 alluvium are considered high, regardless of any natural bonding structure and the associated peak and  
408 softening behaviour.

### 409 410 3.1.3 28 day cured stabilised alluvium

411 The effect of stabilisation was observed to produce shear strengths up to four times higher than those  
412 measured for reconstituted Lanton alluvium, which was accompanied by brittle behaviour upon failure due  
413 to strain localisation and shear plane development. The overall undrained response for the stabilised  
414 alluvium is shown in Figure 9a and 9b. The  $q\text{--}\epsilon_a$  behaviour is generally characterised by work hardening up  
415 to peak conditions, followed by strain softening. Increasing confining stress results in peak  $q$  values being

416 reached at lower  $\epsilon_q$  values; whereby peak values were recorded at approximately 6% strain for samples  
 417 tested at  $p'_0 < 100\text{kPa}$  and 2–3% strain for samples tested at  $p'_0 > 200\text{kPa}$ . The U trends show an initial  
 418 contraction, proportional with the applied confining stress. A peak in U appears to be coincident with the  
 419 onset of yielding followed by a reduction in U. A stable U value is reached beyond  $\epsilon_q = 4\text{--}5\%$ . This  
 420 behaviour is typical of densely cemented soils; whereby for less dense cemented soils, U would be expected  
 421 to continue increasing towards a steady state [16].

422



423

424 Figure 9: (a) Undrained deviatoric stress – strain response; (b) excess pore pressure – deviatoric strain response and (c) drained  
 425 and undrained effective stress paths in the deviatoric stress – mean isotropic stress plane for 28 day cured stabilised Lanton  
 426 alluvium during shear tests.

427

428 For samples tested at  $p'_0 < 200\text{kPa}$ , once U had peaked and started decreasing, they decreased towards  
 429 negative values. Although this behaviour was not observed by [16] on an artificially cemented silty sand,  
 430 it was recorded by Ahnberg [15] for cemented post-glacial Swedish clays. This behaviour is commonly  
 431 observed within dense rocks, whereby the generation of suction occurs close to failure when the material



432 starts to dilate [25] with strain localisation. This U reduction ultimately increased the effective confining  
433 stress and therefore strength.

434 The drained  $q$ - $\varepsilon_q$  response of the 28 day cured GGBS-NaOH cemented alluvium is displayed in Figure 10a.  
435 All samples exhibited non-linear elastic work hardening behaviour up to peak  $q$ , followed by strain  
436 softening. This behaviour became less pronounced with increasing  $p'_0$ ; particularly for  $\geq 400$ kPa. The  
437 magnitude of strains at which yielding occurred also increased with increasing  $p'_0$ .

438 The  $p'_0$  applied to samples during testing appears to influence the  $q$ - $\varepsilon_q$  behaviour of the material. For drained  
439 samples tested at  $p'_0 \leq 200$ kPa, the peak  $q$  and corresponding strains were similar – resembling  
440 overconsolidated behaviour. However, for drained samples tested for  $p'_0 > 400$ kPa the maximum  $q$  values  
441 recorded by samples and their corresponding  $\varepsilon_q$  increased and resembled normally consolidated behaviour.  
442 This was similarly observed by Ahnberg [15] for lime and cement stabilised clays from Sweden, which can  
443 be attributed to the material's vertical yield stress ( $\sigma'_{qp}$ ) (aka quasi preconsolidation pressure) as derived  
444 from one-dimensional consolidation oedometer tests. Ahnberg [15] indicated that  $\sigma'_{qp}$  for cemented soils  
445 depends on the level of cementation within the soil matrix and the magnitude of stress applied to the  
446 material during curing. A value for  $\sigma'_{qp}$  can be estimated based on an empirical correlation with unconfined  
447 compressive strength (UCS), namely  $\sigma'_{qp} = 1.3$ UCS. Sargent et al. [10] undertook UCS and oedometer tests  
448 in accordance with BS1377 [11] on the Lanton soil stabilised with 7.5% GGBS-NaOH after 28 days curing.  
449 UCS values of approximately 1500kPa were recorded, indicating  $\sigma'_{qp} = 430$ kPa. Hence, for samples tested  
450 in this study which had been consolidated to effective stresses  $\geq \sigma'_{qp}$ , a transition in mechanical behaviour  
451 from overconsolidated to normally consolidated behaviour occurred.

452

453



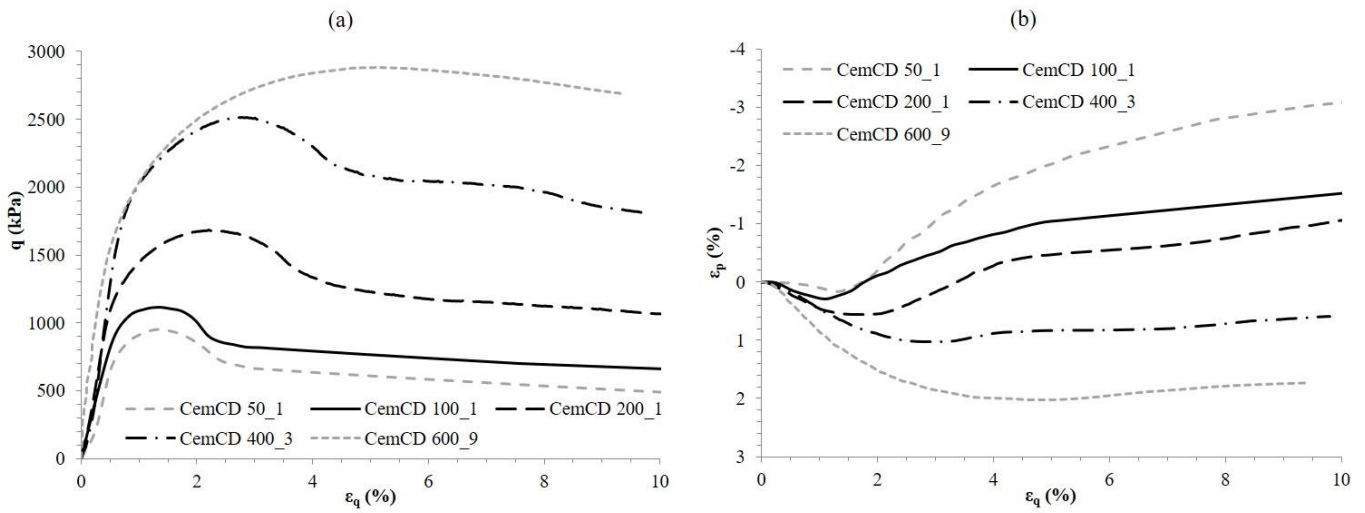


Figure 10: (a) Drained deviatoric stress – shear strain and (b) volumetric – shear strain behaviour of 28 day cured stabilised alluvium samples during shear tests.

$E_{u p'_0}$  and  $E'_{p'_0}$  value ranges for the stabilised Lanton alluvium were recorded as 552–2593MPa and 531–3750MPa, respectively. Evidence for stabilised Lanton alluvium's dilative behaviour during shearing is shown in Figure 10b. Volumetrically, samples experienced a combination of contractional and dilational behaviour. Samples characterised by more dilation were tested at  $p'_0=200$ kPa, whereby the onset of dilation occurred at  $\epsilon_q$  of 1.7%. Negative  $\epsilon_p$  was observed over the  $\epsilon_q$  range of 3–3.5%. Such pronounced dilation corresponds with the softening, due to the breakdown of the newly formed cementitious bonding structure. For samples consolidated to  $p'_0>400$ kPa, their behaviour was predominantly contractional; thereby demonstrating the influence of  $p'_0$  on shearing behaviour. However, at larger  $\epsilon_p$  of 3–5%, samples experienced varying degrees of dilation; albeit no negative  $\epsilon_p$ . This complements the suppressed peak and softening behaviour observed in Figure 10a; whereby work hardening dominates particularly for samples tested at  $p'_0=600$ kPa. Under such stress conditions, particle rearrangement within samples was less permissible compared with at lower  $p'_0$  of 200kPa. Once samples had failed and reached their critical state, no further  $\epsilon_p$  was anticipated as they continued to be sheared. Zero  $\epsilon_p$  was not encountered by samples during testing.

$\Psi$  values for the material ranged between 1.2–3.5°, with higher values obtained for samples tested at lower effective stress conditions. Samples achieving their peak effective stress ratios marked the onset of

474 dilational behaviour. Particularly for samples tested at  $p'_0=200\text{kPa}$ , once the dilation rate peaked at shear  
475 strains of approximately 5%, the degree of dilation and the effective stress ratio reduced.

476

### 477 3.2 Failure Envelopes

478 Using the Mohr's circle at peak strength conditions, the failure envelopes for the three materials have been  
479 determined and provided in Figure 11. The reconstituted alluvium was characterised by average values for  
480 average effective cohesion ( $c'$ ) of  $2.35\text{kPa}$  and effective friction angle ( $\phi'$ ) of  $34.1^\circ$ , whereas the undisturbed  
481 Lanton alluvium exhibited a rather similar average  $\phi'$  of  $32^\circ$  but higher values of  $c'$  equal to  $12\text{kPa}$  as a  
482 result of the internal natural structure. Theoretically, the undisturbed soil ought to possess higher shear  
483 strength properties compared with its reconstituted state, due to the presence of inter-particle bonding  
484 within the soil structure. However, at higher stress levels (i.e.  $\sigma'_n > 200\text{ kPa}$ ) the opposite was observed  
485 whereby that the Mohr-Coulomb failure envelope for the undisturbed soil is positioned beneath that for the  
486 reconstituted soil. This appears emphasised for undrained tests. Considering peak  $q$  values recorded during  
487 undrained tests were generally lower compared with drained tests under identical  $p'_0$  conditions, the  
488 apparent higher strength of reconstituted Lanton alluvium may be attributed to a degree of sample over-  
489 compaction. Some of the soil's bonding-based structure may also have collapsed during transport from the  
490 field to the laboratory.

491 Whilst the untreated alluvium behaved as a typical frictional granular material, the mechanical behaviour  
492 of the cemented alluvium is largely controlled by its cement content. As previously mentioned, strain  
493 localisation and the development of shear failure planes occurred during triaxial compression when stress  
494 conditions closely approached their peak.

495 The applied GGBS-NaOH stabilisation process had a significant impact on the peak strength of the  
496 alluvium, whereby the failure envelope was characterised by an average  $c'$  of  $360\text{kPa}$  as a result of  
497 cementation within the soil matrix, and an average  $\phi'$  of  $37^\circ$ . This suggests that the applied stabilisation  
498 procedure improved not only the cohesive components of the shear strength, but also its frictional  
499 components.

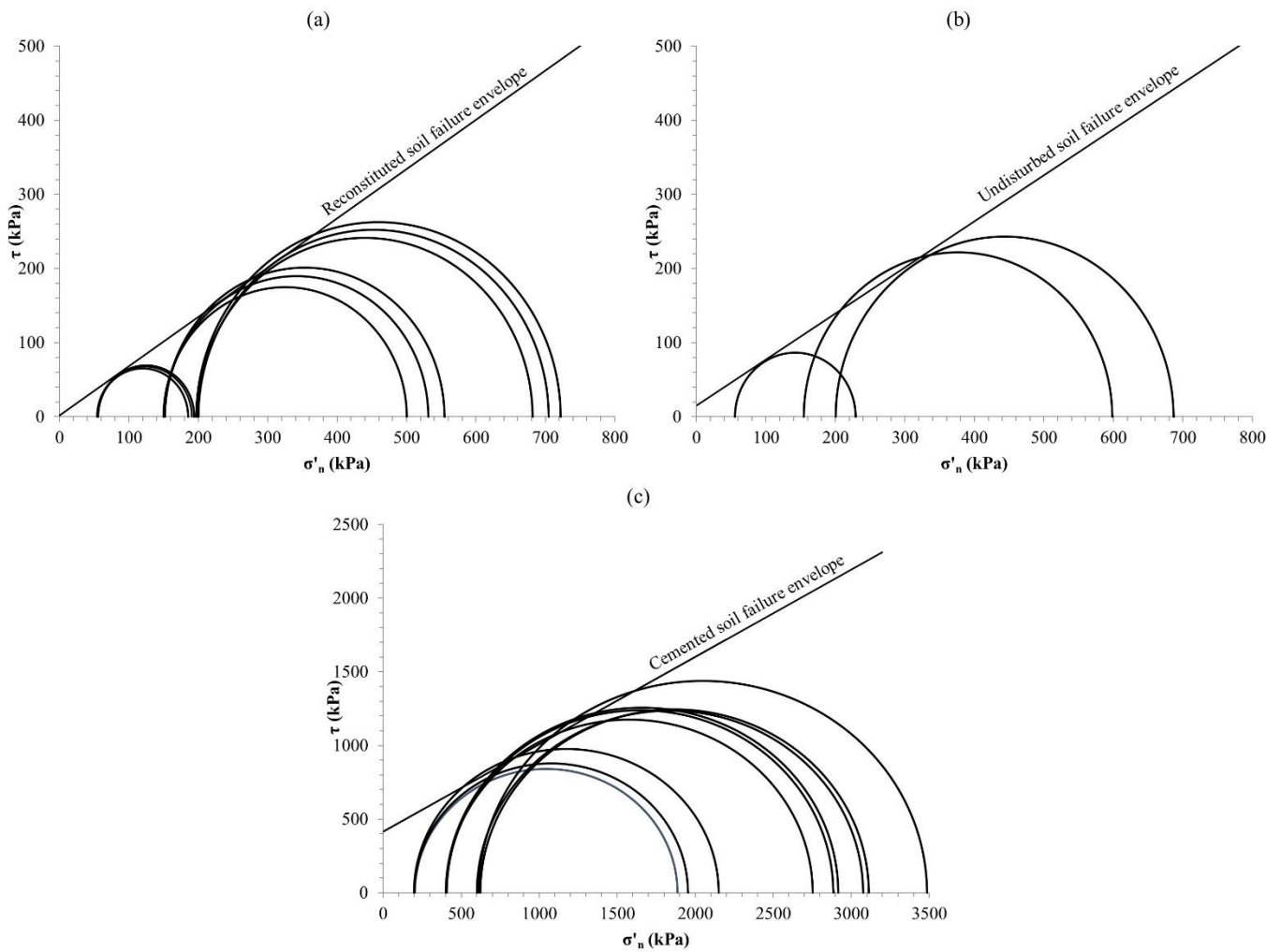


Figure 11: Mohr-Coulomb failure envelopes at peak strength conditions for: (a) reconstituted, (b) undisturbed and (c) 28 day cured stabilised Lanton alluvium.

The effective stress paths followed by the three different materials during both undrained and drained triaxial shearing tests are reported in Figure 12.  $q$  and  $p'$  have been normalised by  $p'_0$  to bring the stress paths together for the purpose of defining a single locus within the  $q/p'_0 - p'/p'_0$  plane. Both reconstituted and undisturbed Lanton alluvium undrained stress paths within  $q-p'$  stress space demonstrate strain hardening with little softening. Drained stress paths followed by all three materials exhibited the 1:3 slope typically expected for drained shear tests. It is possible that the occurrence of localisation within samples during shear testing may have affected the location of the CSL's for the three materials. Therefore, this study provides an estimation of the CSL locations to enable comparisons with different soils.

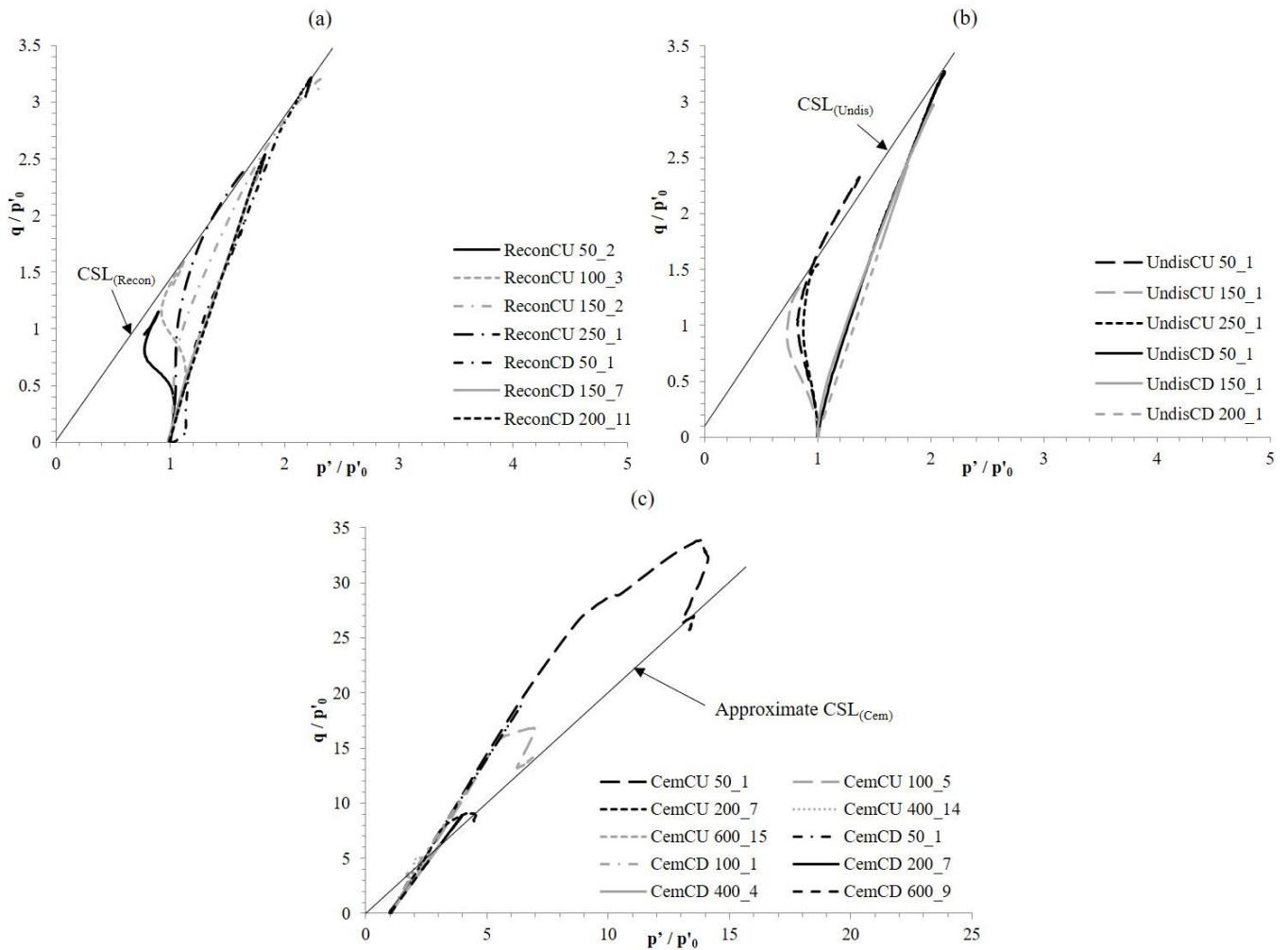


Figure 12:  $p'_0$  normalised drained and undrained effective stress paths for: (a) reconstituted, (b) undisturbed and (c) 28 day cured stabilised Lanton alluvium.

The CSL's for all three materials pass through the origin, as typically expected for frictional granular soils. Per Figure 12a, the average gradient ( $M$ ) measured for the estimated location of  $CSL_{(Recon)}$  was 1.42, deriving a  $\phi' = 35^\circ$ . Whereas in Figure 12b for the undisturbed alluvium, an  $M$  value of 1.37 was measured for the estimated location of the  $CSL_{(Undis)}$ , deriving  $\phi' = 34^\circ$ . By examining the stress path data for the stabilised Lanton alluvium in Figure 12c, the estimated  $CSL_{(Cem)}$  has a steeper gradient compared with the reconstituted and undisturbed Lanton alluvium, thereby giving a higher  $M$  value of 1.88. This provides an estimate of  $\phi' = 40^\circ$ . Whilst the CSL estimates for effective friction angle are similar to those measured from peak Mohr circles for the reconstituted and undisturbed Lanton alluvium, there seems to be some disparity regarding the friction angle estimates for the stabilised alluvium. This is largely attributed to sample variability regarding level of cementation.

526 Whilst  $p'$  generically influences the shear stiffness of soils, it appears less significant for the stabilised  
527 alluvium at  $p' \leq 200\text{kPa}$ . Peak  $q$  values for undrained samples were similar at  $p'_0$  values of 50 and 100kPa.  
528 For undrained tests undertaken at  $p'_0 > 400\text{kPa}$ , increases in peak  $q$  and a change in shape of the effective  
529 stress paths in  $q$ - $p'$  stress space were observed. The normalisation of effective stress paths in Figure 11  
530 shows that samples consolidated to higher  $p'_0$  achieved higher peak  $q$ . Per Muir Wood [26], this proved  
531 useful in defining a single locus for the stabilised material within the  $q / p'_0 - p' / p'_0$  plane.

532 The shapes of undrained effective stress paths varied according to the level of effective confining stress.  
533 For samples tested at  $p'_0 \leq 200\text{kPa}$ , stress paths followed a 1:3 slope similar to drained tests until they  
534 reached their yielding point when a sharp phase transformation occurred. The stress paths then followed  
535 the failure envelope until sample rupture and failure occurred. For undrained stress paths taken by samples  
536 tested at confining stresses  $\geq 400\text{kPa}$ , their shapes resemble those typically expected for soils which  
537 predominantly experience work hardening with limited softening. Once these samples started to reach  
538 advanced stages of yielding and their corresponding stress paths had reached their failure envelopes, a phase  
539 transformation occurred.  $p'$  increased whilst  $q$  stabilised. Once stress paths reached their peak strength (i.e.  
540 defining the failure envelope),  $q$  started to decrease. It is thought that this resulted in the stress paths coming  
541 down to meet the CSL. However, the stress paths only followed the CSL briefly, as  $q$  often suddenly  
542 decreased due to brittle rupturing and volumetric increase within the samples.

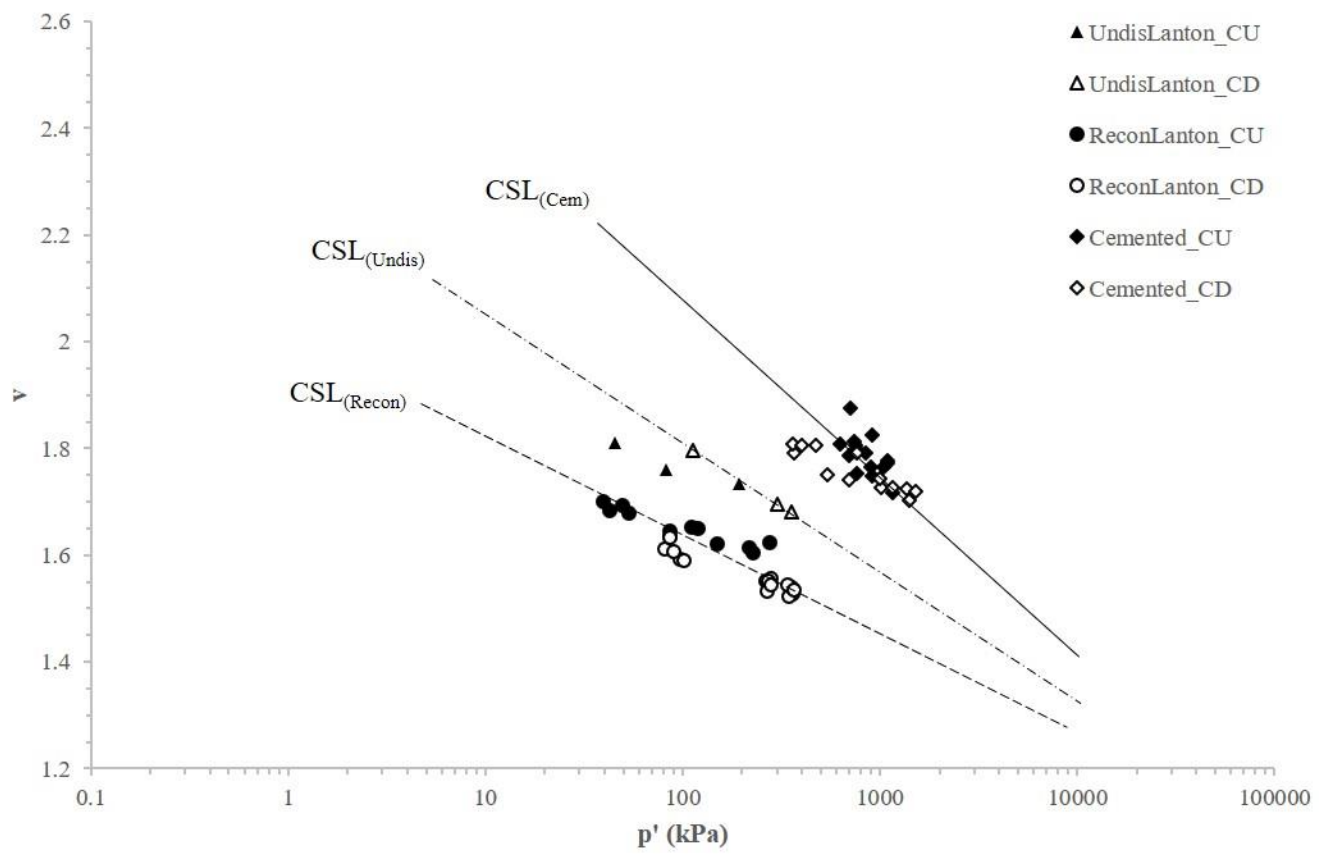
543

### 544 3.3 Ultimate State Locus in the Volumetric Stress Plane

545 The end points of stress paths followed by all samples tested in the typical specific volume versus logarithm  
546 of mean effective stress ( $v - \ln p'$ ) are reported in Figure 13. The end points are highlighted to determine  
547 the likely location of the CSL's for the reconstituted, undisturbed and stabilised Lanton alluvium. It should  
548 be noted that the occurrence of strain localisation or non-homogeneity of deformation within the tested  
549 samples can prevent the determination of the exact location of the critical state line. Nevertheless, a general  
550 approximation of the position of the ultimate state locus for the three materials can still be obtained. The  
551 data plotted in Figure 13 shows how the compression curve end points and the CSL's for the GGBS-NaOH

552 stabilised alluvium samples plot well above the respective data for the reconstituted and undisturbed  
 553 samples.

554



555

556 Figure 13: Possible CSL surfaces for reconstituted, undisturbed and stabilised Lanton alluvium in the  $v - \ln p'$  stress plane.

557

558 It is clear that the presence of internal structure, either in the form of natural post-sedimentation structure  
 559 or artificial cementation, results in an upward movement of the CSL. Such movement is greater for the  
 560 stronger structure provided by the GGBS-NaOH stabilisation. However, it is difficult to comment on the  
 561 relationship between the slope of the CSL's, due to the relatively limited range of mean effective stress and  
 562 the uncertainty relating to strain localisation and inhomogeneity of deformation. According to critical state  
 563 soil mechanics theory, it may be assumed that the ultimate compression locus for the undisturbed and  
 564 stabilised Lanton alluvium will converge with the intrinsic compression line for the Lanton alluvium at  
 565 very high stress levels. The data trends shown in Figure 13 appears to generally corroborate such an  
 566 assumption, based on the mean effective stresses experienced by the samples tested. However, Todisco and  
 567 Coop [27] determined that soils characterised by more complex particle size distributions and mineralogies

568 may not exhibit convergence behaviour. Given the cement bonding-based structure and thus more complex  
569 mineralogy of the stabilised Lanton alluvium due to the inclusion of the GGBS-NaOH binder and  
570 cementitious gels, further triaxial testing involving higher strains and effective confining stresses would be  
571 required to determine whether convergence will occur.

572

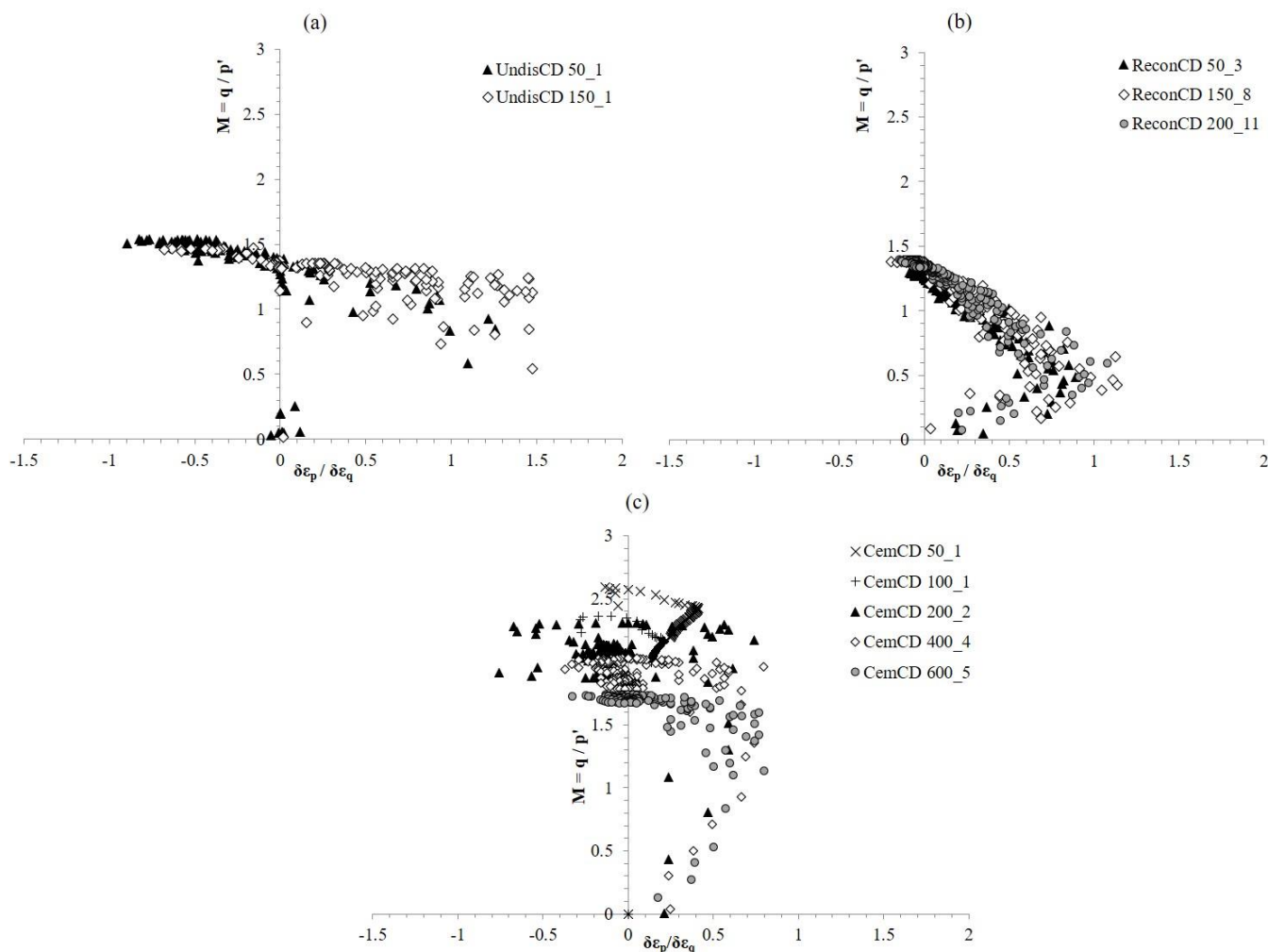
### 573 3.4 Stress – Dilatancy Relationship

574 The stress-dilatancy relationships for the three investigated materials are reported in Figure 14 to allow a  
575 direct comparison among the materials and understand the influence of the presence of both natural and  
576 artificial cemented structure. The stress-dilatancy behaviour of reconstituted samples is displayed in Figure  
577 14b, whereby all samples display frictional behaviour. They compress to ultimately reach similar critical  
578 state  $M$  values of 1.3–1.4, with some limited dilation associated with reaching the peak strength ratio. The  
579 data seems to follow the typical linear trend between stress ratio and incremental strain ratio, after the elastic  
580 component of deformation becomes negligible. The undisturbed Lanton alluvium samples also reached  
581 critical state ratio ( $M$ ) values (i.e.  $q / p'$ ) of 1.3–1.4, although they experienced larger dilation during testing  
582 (Figure 14a). The relationship between stress ratio and strain ratio seems to be governed by a much flatter  
583 line if compared with the reconstituted Lanton alluvium. This is thought to be a consequence of internal  
584 structure and some natural bonding between the soil particles.

585 The presence of strong cementitious bonding within the stabilised Lanton alluvium results in a unique  
586 critical state stress ratio, which appears to decrease with the applied stress level as shown in Figure 14c.  
587 The strength contribution provided by the cementitious bonding is generally stress dependent and becomes  
588 less significant as the testing confining stress increases. Interestingly, for all of the samples tested, the  
589 dilatancy stress- relationship is initially very flat (gradient close to zero), which confirms that the peak  
590 strength of the stabilised alluvium samples is not related to a frictional mechanism, but largely governed  
591 by the artificial cementation. After a peak rate, the dilation reduces together with the stress ratio which  
592 agrees with the observations of Rios et al. [16] on artificially cemented soils and Coop and Wilson [28] on  
593 sandstones. For the stabilised soil, the ultimate value of the peak strength ratio is considerably higher than

594 that of the reconstituted and undisturbed alluvium. This suggests that during shearing, the stabilised material  
 595 does not evolve in the original non-cemented reconstituted alluvium.

596



597

598 Figure 14: Stress-dilatancy relationship for (a) reconstituted, (b) undisturbed and (c) 28 day cured stabilised Lanton alluvium.

599

### 600 3.5 Shear stiffness

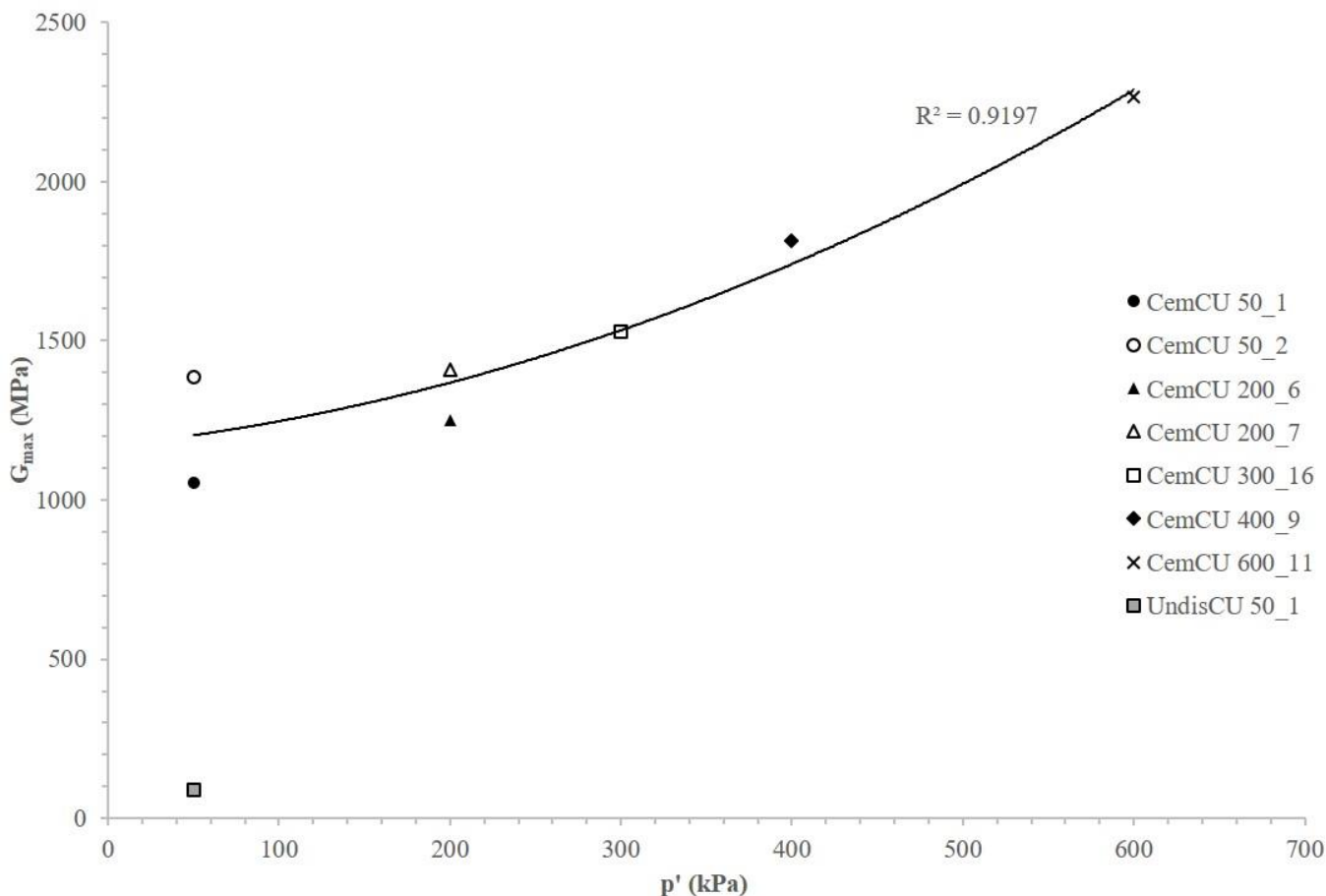
#### 601 3.5.1 Characterisation of the Small Strain Stiffness

602 Bender elements and measurements from local instrumentation attached to the middle third of samples were  
 603 used to assess the relationship between the initial shear stiffness ( $G_{\max}$ ) and the applied  $p'_0$ . An average  
 604  $G_{\max}$  value of 89MPa was obtained from bender element measurements performed on samples consolidated  
 605 to a  $p'_0$  of 50kPa prior to shearing. For the stabilised alluvium, bender element and local strain  
 606 measurements indicated  $G_{\max}$  values to range between 1053 and 1813MPa for the  $p'_0$  range of 50–600kPa.



607 The relationship between  $G_{max}$  and the applied confining stress for the three investigated materials are  
 608 reported in Figure 15. While the derivation of such a relationship for the reconstituted and undisturbed  
 609 Lanton alluvium is beyond the scope of this paper, the results of Figure 15 demonstrate that the proposed  
 610 stabilisation method provides an approximate 13 fold increase in initial shear stiffness.

611



612

613 Figure 15: Relationship between  $G_{max}$  and initial mean effective stress for undisturbed and 28 day cured stabilised Lanton  
 614 alluvium.

615

616 Figure 15 shows that the value of  $G_{max}$  for the stabilised Lanton alluvium is not proportional to the applied  
 617 confining stress. Variability of the data does not assist in this situation, but it may appear that, for lower  
 618 values of mean isotropic stress (i.e. <200kPa), the  $G_{max}$  is constant or may even decrease with increasing  
 619 mean isotropic stress. This was similarly observed by Verastegui-Flores and Van Impe [29] for a cemented  
 620 kaolin soil. In this stress range, the structure of the stabilised material is entirely governed by the  
 621 cementation and an eventual reduction in shear stiffness ( $G$ ) with stress level may be associated with a  
 622 collapse of the cemented soil structure. For isotropic stress levels greater than 200kPa, the  $G_{max}$  value

623 increases as it would be expected for non-cemented frictional soils. This suggests that the frictional nature  
624 of the soil matrix is activated for these stress levels.

625

### 626 3.5.2 Degradation of shear stiffness during shearing

627 The measured  $G$  degradation behaviour for the undisturbed and stabilised Lanton alluvium is presented in  
628 Figure 16, whereby  $G$  values were normalised with respect to the measured  $G_{\max}$  value. Data scatter is  
629 observed within the small strain range, which may be due to the slightly lower resolution of stiffnesses  
630 calculated from the axial and radial LVDT's local strain gauges compared with bender element  
631 measurements. For the undisturbed Lanton alluvium,  $G$  degrades significantly at small strains. The  
632 degradation is much more rapid if compared with highly structured cohesive soils such as London Clay, as  
633 tested by Gasparre [19] whose initial structure and highest stiffnesses are retained up to shear strains of  
634 approximately 0.01%.

635 For the majority of stabilised alluvium samples, the onset of  $G$  degradation during compression occurs at  
636 approximately 1% shear strain. The shear strain levels at which the shear stiffness of the cemented samples  
637 starts to degrade is approximately three orders of magnitude higher than those measured for the undisturbed  
638 alluvium. This highlights the level of improvement in mechanical behaviour provided by the addition of  
639 the GGBS-NaOH binder and 28 days curing.

640

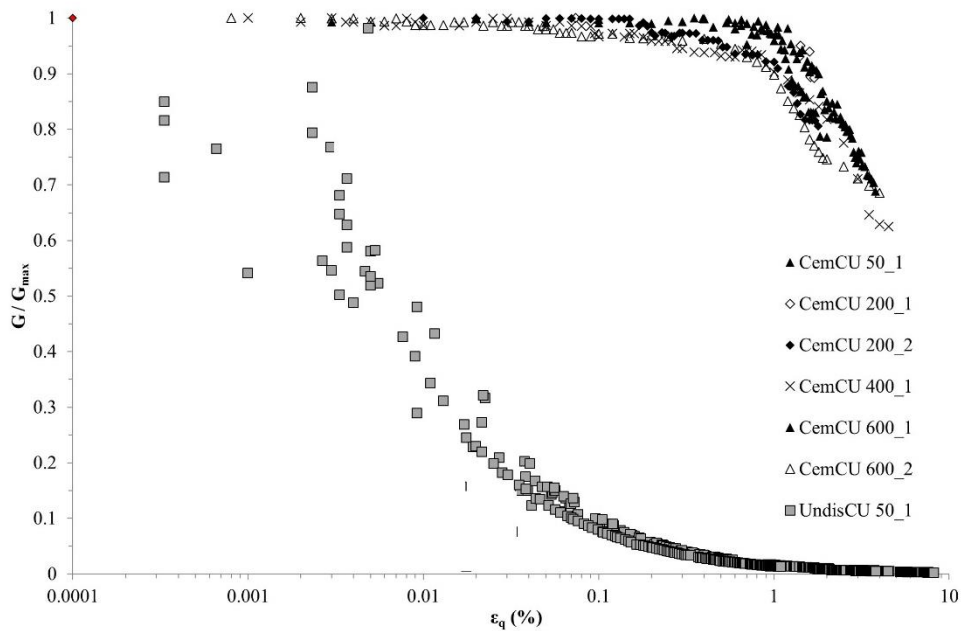


Figure 16: Normalised shear stiffness degradation curves for the undisturbed and 28 day cured stabilised Lanton alluvium.

#### 4.0 Conclusions

An extensive experimental triaxial testing programme was undertaken on reconstituted, undisturbed and stabilised Lanton alluvium samples to characterise the improvement in mechanical behaviour provided by the precipitation of cementitious gels (most likely C-(N)-A-S-H) derived from a new low carbon GGBS-NaOH binder [21]. Findings presented by Sargent et al. [10] informed the work presented in this paper, which revealed that the engineering performance of the GGBS-NaOH binder at a dosage of 7.5% was comparable to using a 10% dosage of CEM-I, thereby meeting minimum strength requirements defined by the EuroSoilStab [12] standard. All cemented samples had a controlled binder dosage of 7.5% (i.e. 107kg m<sup>-3</sup>). The analysis of the experimental results has revealed the following insights:

- The use of the GGBS-NaOH binder proved successful in significantly increasing the shear strength of the initially soft and sensitive Lanton alluvium soil by a factor of 13 after 28 days curing. The relationship between initial shear stiffness and effective stress level is non-linear: the stiffness appears to be chiefly governed by the cemented structure of the material for low stress levels up to 200kPa. The initial stiffness of the cemented soil was also significantly improved, which only started to degrade at shear strain levels of 1% - approximately three orders of magnitude higher than the untreated undisturbed alluvium.

- 660 • GGBS-NaOH stabilised samples exhibited higher values of maximum dilation for the same  
661 confining stresses. Such pronounced dilation corresponds with the onset of softening, due to the  
662 breakdown of the newly formed internal cementitious bonding structure.
- 663 • The peak strength of the stabilised Lanton alluvium was less influenced by the frictional mechanism  
664 but largely governed by the artificial cementation. Only after the peak rate is reached, the dilation  
665 reduces together with the stress ratio to eventually reach their ultimate values.
- 666 • Possible locations for the untreated and GGBS-NaOH cemented alluvium's critical state lines have  
667 been defined in the mean effective stress and  $v - \ln p'$  stress planes. The CSL surfaces for the  
668 reconstituted and undisturbed soil are indicated to be approximately in parallel with each other in  
669 the  $v - \ln p'$  stress plane. The stress paths for the cemented alluvium were akin to heavily over-  
670 consolidated soils or soft rocks, defining a new CSL surface located above those for the natural soil.

671 Further research is required for characterising the mechanical behaviour of the GGBS-NaOH cemented soft  
672 alluvial soils under higher effective confining pressures, with focus on fatigue, creep and response to  
673 dynamic and cyclic loading conditions associated with earthquake phenomena and modern engineering  
674 infrastructure such as high-speed railways.

675 For soils that are softer and more problematic compared with Lanton alluvium, higher binder dosages (i.e.  
676  $\geq 10\%$ ) may be required to achieve high strengths. Additionally, the GGBS-NaOH ratio will require careful  
677 customisation for individual projects, whereby higher NaOH concentrations would be required to  
678 effectively stabilise soils characterised by a low pH. However, using high concentrations of NaOH will  
679 result in the binder becoming less environmentally and financially sustainable. The mineralogy / chemistry  
680 of a soil (i.e. organic and sulphate contents) being considered for stabilisation must be investigated prior to  
681 selecting the binder to be used on site. Failure to do so may result in ineffective stabilisation and potentially  
682 worsen ground conditions in the long term due to the formation of structurally unfavourable minerals such  
683 as ettringite.

686 **References**

- 687 [1] Sargent, P., 2014. Alkali activated mixtures for soil stabilisation, in Pacheco-Torgal, F., Labrincha,  
688 J., Leonelli, C., Palomo, A. and Chindaprasit, P. (Eds.), Handbook of alkali activated cements,  
689 mortars and concretes. Woodhead Publishing.
- 690 [2] Davidson, L. K., Demirel, T. and Handy, R. I., 1965. Soil Pulverization and Lime Migration in Soil  
691 Lime Stabilisation. Highway Research Record. 92, 103-126.
- 692 [3] Tutumluer, E., 2012. Short course notes for Geotechnical Aspects of Pavement Design and  
693 Construction – ASCE GeoCongress 2012 “State of the Art and Practice in Geotechnical  
694 Engineering”, 25 – 29th March 2012, Oakland, CA, USA.
- 695 [4] Ghadir, P. and Ranjbar, N., 2018. Clayey soil stabilization using geopolymer and Portland cement.  
696 Construction and Building Materials. 188, 361-371.
- 697 [5] McLellan, B. C., Williams, R. P., Lay, J., van Riessen, A. and Corder, G. D., 2011. Costs and carbon  
698 emissions for geopolymer pastes in comparison to ordinary portland cement. Journal of Cleaner  
699 Production. 19, 1080-1090. Doi: 10.1016/j.jclepro.2011.02.010.
- 700 [6] Cristelo, N., Glendinning, S. and Teixeira Pinto, A., 2011. Deep soft soil improvement by alkaline  
701 activation. Proceedings of the Institution of Civil Engineers, Ground Improvement. 164 (2), 73-82.  
702 Doi: 10.1680/grim.900032.
- 703 [7] Sargent, P., Hughes, P. N., Rouainia, M. and White, M., 2013. The use of alkali activated waste  
704 binders in enhancing the mechanical properties and durability of soft alluvial soils. Engineering  
705 Geology. 152, 96-108. Doi: 10.1016/j.enggeo.2012.10.013.
- 706 [8] Habert, G., d’Espinoze de Lacaillerie, J. B. and Roussel, N., 2011. An environmental evaluation of  
707 geopolymer based concrete production: reviewing current research trends. Journal of Cleaner  
708 Production. 19, 1229-1238. Doi: 10.1016/j.clepro.2011.03.012.
- 709 [9] Bernal, S. A., 2014. The resistance of alkali-activated cement-based binders to carbonation. In:  
710 Pacheco-Torgal, F., Labrincha, J., Leonelli, C., Palomo, A. and Chindaprasit, P. (Eds.), Handbook  
711 of Alkali-activated Cements, Mortars and Concretes. Woodhead Publishing. ISBN 978-1-78242-  
712 276-1.
- 713 [10] Sargent, P., Hughes, P. N. and Rouainia, M., 2016. A new low carbon cementitious binder for  
714 stabilising weak ground conditions through deep soil mixing. Soils and Foundations (The Japanese  
715 Geotechnical Society). 56 (6), 1021-1034. Doi: 10.1016/j.sandf.2016.11.007.
- 716 [11] BSI, 1990. BS: 1377 Incorporating Amendment No. 1, Methods of test for Soils for Civil  
717 Engineering Purposes. British Standards Institution, Milton Keynes.

- 718 [12] EuroSoilStab, 2002. Development of design and construction methods to stabilise soft organic soils:  
719 Design guide soft soil stabilisation. CT97-0351. Project No.: BE 96-
- 720 [13] Ge, L., Wang, C-C., Hung, C-W., Liao, W-C. and Zhao, H., 2018. Assessment of strength  
721 development of slag cement stabilized kaolinite. *Construction and Building Materials*. 184, 492-  
722 501.
- 723 [14] USGS, 2015. Volcanic Ash Impacts & Mitigation – Water Supply. [online]. Available at:  
724 <[https://volcanoes.usgs.gov/volcanic\\_ash/water\\_supply.html](https://volcanoes.usgs.gov/volcanic_ash/water_supply.html)>. Last accessed: 7<sup>th</sup> September 2018.
- 725 [15] Ahnberg, H., 2007. On yield stresses and the influence of curing stresses on stress paths and strength  
726 measured in triaxial testing of stabilized soils. *Canadian Geotechnical Journal*. 44, 54-66. Doi:  
727 10.1139/T06-096.
- 728 [16] Rios, S., Viana da Fonseca, A. and Baudet, B. A., 2014. On the shearing behaviour of an artificially  
729 cemented soil. *Acta Geotechnica*. 9, 215-226. Doi: 10.1007/s11440-013-0242-7.
- 730 [17] Hansson, T., Parry, L., Graham, M., Troughton, V. and Eriksson, H., 2001. Limix: a deep dry mixing  
731 system used at Channel Tunnel Rail Contract 440. *Proceedings of Underground Construction 2001*  
732 *Symposium and Exhibition*, London. Institute of Materials, Minerals and Mining, London.
- 733 [18] American Society for Testing and Materials (ASTM), 2008. Designation: D 4543-08 Standard  
734 Practices for Preparing Rock Core as Cylindrical Test Specimens and Verifying Conformance to  
735 Dimensional and Shape Tolerances. *Annual Book of ASTM Standards*. 4.08, West Conshocken: Pa.
- 736 [19] Gasparre, A., 2005. Advanced laboratory characterisation of London Clay. PhD thesis. Department  
737 of Civil and Environmental Engineering, Imperial College London.
- 738 [20] Rees, S., Le Compte, A. and Snelling, K., 2013. A new tool for the automated travel time analyses  
739 of bender element tests. *Proceedings of the 18<sup>th</sup> International Conference on Soil Mechanics and*  
740 *Geotechnical Engineering*, Paris 2013. Technical Committee 212. 2843-2846.
- 741 [21] Sargent, P., 2015. Secondary minerals to replace cement in stabilising an alluvium. Ph.D. thesis,  
742 Newcastle University, UK.
- 743 [22] Bowles, J. E., 1977. *Foundation Analysis and Design*. 2nd edition, McGraw-Hill, New York. ISBN  
744 10: 0070067503.
- 745 [23] Obrzud, R. F., 2010. On the use of the Hardening Soil Small Strain model in geotechnical practice,  
746 in *Numerics in Geotechnics and Structures*. Eds Zimmerman et al., Elsevier, Lausanne.
- 747 [24] Carter, M. and Bentley, S. P., 1991. *Correlations of soil properties*. Pentech Press Ltd., ISBN 0-7273-  
748 0317-1.
- 749 [25] Mesri, G., Jones, R. A. and Adachi, K., 1972. Annual report on Influence of Pore Water Pressure  
750 on the Engineering Properties of Rock. Department of Civil Engineering, University of Illinois,

- 751 Urbana, Illinois, USA. [online]. Available at: <<http://www.dtic.mil/dtic/tr/fulltext/u2/740169.pdf>>.  
752 Last accessed: 10th June 2014.
- 753 [26] Muir Wood, D., 1990. Soil Behaviour and Critical State Soil Mechanics. Cambridge University  
754 Press. ISBN: 0521332494.
- 755 [27] Todisco, M. C. and Coop, M. R., 2016. Normalisation techniques for slowly-converging soils.  
756 Procedia Engineering. 158, 110-115. Doi: 10.1016/j.proeng.2016.08.414.
- 757 [28] Coop, M. R. and Wilson, S. M., 2003. On the behaviour of Hydrocarbon Reservoir Sands and  
758 Sandstones. Journal of Geotechnical Engineering, ASCE. 129 (11), 1010-1019.
- 759 [29] Verastegui Flores, R. D. and Van Impe, W. F., 2009. Stress-strain behaviour of artificially cemented  
760 Kaolin clay. Proceedings of the 17<sup>th</sup> International Conference on Soil Mechanics and Geotechnical  
761 Engineering, Hanza, M. et al. (Eds). 283-286.